On the nature of anomalous rectification in thalamocortical neurones of the cat ventrobasal thalamus *in vitro*

Stephen R. Williams, Jonathan P. Turner, Stuart W. Hughes and Vincenzo Crunelli*

Physiology Unit, School of Molecular and Medical Biosciences, University of Wales Cardiff, Museum Avenue, Cardiff, CF1 1SS, UK

1. Intracellular sharp electrode current clamp and discontinuous single electrode voltage clamp recordings were made from thalamocortical neurones ($n = 57$) of the cat ventrobasal thalamus in order to investigate the mechanisms underlying anomalous rectification.

2. Under current clamp conditions, voltage–current (V–I) relationships in a potential range of −55 to −110 mV demonstrated anomalous rectification with two components: fast rectification, which controlled the peak of negative voltage deviations, and time-dependent rectification. Time-dependent rectification was apparent as a depolarizing sag generated during the course of negative voltage deviations, was first formed at potentials in the range −60 to −70 mV, and was sensitive to 3 mM Cs^+ ($n = 6$). Similarly, under voltage clamp conditions, instantaneous and steady-state I–V relationships demonstrated anomalous rectification. A slowly activating inward current with an activation threshold in the range of −65 to −70 mV formed time-dependent rectification. This current was sensitive to Cs^+ (3 mM) ($n = 3$) and had properties similar to the slow inward mixed cationic current (I_h).

3. 4-(*N*-Ethyl-*N*-phenylamino)-1,2-dimethyl-6-(methylamino)-pyrimidinium chloride (ZD 7288) (100–300 μM) irreversibly blocked time-dependent rectification mediated by I_h ($n = 23$ of 25 neurones), and led to a hyperpolarization of the resting membrane potential (6·8 ± 0·5 mV). In the presence of ZD 7288, V–I and I–V relationships exhibited fast anomalous rectification, first activated from potential more negative than −80 mV.

4. Ba^{2+} (100 μM) ($n = 8$), in the continuous presence of ZD 7288, reversibly linearized peak V–I and instantaneous I–V relationships over a potential range of −70 to −120 mV, and led to a membrane depolarization (13·3 ± 4·2 mV) or tonic inward current (192 ± 36 pA).

5. The co-application of ZD 7288 and Ba^{2+} revealed a depolarizing sag in negative voltage deviations under current clamp conditions, or a large inward current with kinetics two to three times slower than those of I_h under voltage clamp conditions. This novel form of time-dependent rectification was first apparent at potentials more negative than about −85 mV, was sensitive to 5 mM Cs^+ ($n = 4$), and is termed $I_{h,slow}$. $I_{h,slow}$ tail currents reversed between −65·3 and −56·6 mV (with potassium acetate electrodes, $n = 3$) or −57·6 and −50·3 mV (with KCl electrodes, $n = 3$).

6. Computer simulations confirmed that the pattern of anomalous rectification in thalamocortical neurones of the cat ventrobasal thalamus is mediated by the concerted action of I_h and a Ba^{2+}-sensitive current with properties similar to an inwardly rectifying K^+ current (I_{KIR}).

The importance of anomalous rectification and so the underlying hyperpolarization-activated membrane currents to the electrophysiological behaviour of thalamocortical (TC) neurones has been demonstrated by the involvement of a slow inward mixed cationic current (I_h) (McCormick & Pape; 1990; Soltesz, Lightowler, Leresche, Jassik-Gerchenfeld, Pollard & Crunelli, 1991) in the generation and control of intrinsic and network-driven oscillatory activity (McCormick & Pape, 1990; Soltesz *et al.* 1991; Steriade, Curró Dossi & Nuñez, 1991; Tóth & Crunelli, 1992; Steriade, McCormick & Sejnowski, 1993) and the formation and control of slow after-hyperpolarizing potentials (McCormick & Pape, 1990).

* To whom correspondence should be addressed.

Furthermore, the voltage dependence and kinetics of activation of I_h indicates that this current will be activated by inhibitory postsynaptic potentials and influence the rate of potential repolarization (cf. McCormick & Pape, 1990). Despite the pivotal role of hyperpolarization-activated currents in the formation of TC neurones electroresponsiveness, investigations have been restricted to the dorsal lateral and medial geniculate nuclei (McCormick & Pape, 1990; Soltesz *et al.* 1991), and the electrophysiological properties of TC neurones of these thalamic nuclei have been considered to be representative of the thalamus in general. Recently, however, it has been observed that neurones of the dorsal and ventral divisions of the medial geniculate nucleus exhibit differences in the degree of I_h-mediated rectification (Hu, 1995). Furthermore, *in vivo* recordings have suggested that both intrinsic and network-generated oscillatory activity of TC neurones may be more robust in other areas of the thalamus, for example, in the ventrobasal (VB) thalamus (Steriade *et al.* 1991), raising the possibility that the properties of hyperpolarization-activated current(s) may be different in this part of the thalamus.

In addition, the possible expression of hyperpolarization-activated currents other than I_h in TC neurones has not been adequately investigated, partly because the pharmacological agents used to block I_h are not specific for this current but block other membrane currents such as the inwardly rectifying K^+ current (I_{KIR}) (Hagiwara, Miyazaki & Rosenthal, 1976; Gay & Stanfield, 1977; Hagiwara, Miyazaki, Moody & Patlak, 1978; Standen & Stanfield, 1978; Constanti & Galvan, 1983; Uchimura, Cherubini & North, 1989; Sutor & Hablitz, 1993; Womble & Moises, 1993; Nisenbaum & Wilson 1995). The development of bradycardiac agents that have been shown to block I_f in cardiac cells (VanBogaert, Goethals & Simoens, 1990; BoSmith, Briggs & Sturgess, 1993), however, has recently allowed the demonstration of a specific block of I_h in TC neurones of the guinea-pig dorsal lateral geniculate nucleus (Pape, 1994).

Using an *in vitro* slice preparation of the cat VB thalamus we report that the anomalous rectification properties of TC neurones are complex, and are characterized by fast and slow components. Following the specific blockade of I_h with 4-(*N*-ethyl-*N*-phenylamino)-1,2-dimethyl-6-(methylamino)-pyrimidinium chloride (ZD 7288), we have observed the presence of fast rectification sensitive to Ba^{2+}, in a manner consistent with the activation of an inwardly rectifying K^+ current. The blockade of this K^+ current has revealed the presence of a non-inactivating, inward current with very slow activation kinetics that may represent a distinct membrane current. Some of these results have been published in a preliminary form (Williams & Crunelli, 1996).

METHODS

Slice preparation and recording procedures

Young adult male and female cats (1–1·5 kg) were deeply anaesthetized with a mixture of O_2 and NO_2 (2:1) and 1% halothane. The top of the skull was exposed, a wide craniotomy performed and the meninges were removed. The animals were killed by a coronal cut at the level of the inferior colliculus, and, following transection of the optic tracts, the brain was removed and submerged in ice-cold (1–4 °C), oxygenated (95% O_2–5% CO_2) modified Krebs medium containing (mM): KCl, 5; KH_2PO_4, 1·25; $MgSO_4$, 5; $CaCl_2$, 1; $NaHCO_3$, 16; glucose, 10; sucrose, 250. Slices were left in the storage chamber for at least 1 h before being transferred to a recording chamber where they were perfused with a continuously oxygenated (95% O_2–5% CO_2) medium of similar composition, but with 1 mM $MgSO_4$ plus 2 mM $CaCl_2$ replacing the 5 mM $MgSO_4$ plus 1 mM $CaCl_2$, respectively. Other details of the preparation and maintenance of cat VB slices were identical to those fully described in the accompanying paper (Turner, Anderson, Williams & Crunelli, 1997) except for the following procedures. In experiments where $BaCl_2$, $NiCl_2$ or $ZnCl_2$, but not CsCl, were ultimately to be added to the recording medium, KH_2PO_4 was omitted and $MgSO_4$ was replaced with equimolar $MgCl_2$. In each experiment the recording medium contained a combination of the following excitatory and inhibitory amino acid receptor antagonists: 6-cyano-7-nitroquinoxaline-2,3-dione (CNQX) (20 μM), 1-(4-amino-phenyl)-4-methyl-7,8-methylene-dioxy-5H-2,3-benzodiazepine (GYKI 52466) (100 μM), D,L-2-amino-5-phosphonovaleric acid (APV) (100 μM), (5*R*,10*S*)-(+)-5-methyl-10,11-dihydro-5H-dibenzo[*a*,*d*]-cyclohepten-5,10-imine hydrogen maleate (MK 801) (10 μM), bicuculline methiodide (30 μM) and *P*-(3-aminopropyl)-*P*-diethoxymethl-phosphinic acid (CGP 35348) (500 μM).

Intracellular sharp electrode recordings were made with thin-walled glass microelecetrodes (GC 120TF; Clark Electromedical Instruments, Reading, UK) filled with 1 M potassium acetate, 2% biocytin dissolved in 1 M potassium acetate or 3 M potassium chloride (resistance 20–50 MΩ). Potentials and currents were recorded with an Axoclamp-2A amplifier (Axon Instruments), configured in bridge balance or discontinuous single electrode voltage clamp (dSEVC) mode. When entering dSEVC mode the amplifier was initially configured in discontinuous current clamp mode and using the procedures detailed by Finkel & Redman (1984) dSEVC mode was achieved. The headstage output was continuously monitored to ensure adequate settling time. Sampling frequencies ranged between 2·5 and 3·5 kHz and the amplifier gain ranged between 0·3 and 0·5 nA mV^{-1}. Potentials were stored on a Biologic DAT recorder (Intracel, Royston, UK). Data were subsequently filtered (DC to 0·5–30 kHz), digitally sampled, and analysed with a microcomputer running pCLAMP software (Axon Instruments). For recordings made under current clamp conditions, voltage–current (*V–I*) relationships were constructed from a membrane potential in the range −55 to −65 mV, where positive current steps failed to evoke a low-threshold Ca^{2+} potential. Voltage deviations were measured at peak amplitude and 10 ms before the offset (steady state) of the potential, and input conductance was calculated as the reciprocal of the apparent input resistance measured in the steady state. Under voltage clamp conditions, *V–I* relationships were constructed from a holding potential of −50 to −55 mV under control conditions and from a holding potential of between −50 and −70 mV for the analysis of $I_{h,slow}$. Under voltage clamp conditions, the instantaneous current was measured at 50 ms following the onset of voltage command steps and the steady-state current at 10 ms before the offset of voltage command steps. The membrane currents were averaged over two to three consecutive traces. Input conductance was calculated from the equation $g_{in} = I_S(V - V_H)$, where I_S is steady-state current, V is command potential and V_H is holding potential. The activation kinetics of

membrane currents were estimated using the exponential fitting routine offered by pCLAMP software: fits were started 50 ms following the onset of voltage command steps to allow settling of capacative artifacts. Both the simplex and Chebyshev algorithm were used and found to produce similar results.

Neurones in the cat VB were identified as TC neurones by electrophysiological procedures or morphological analysis of biocytin-injected neurones (Turner *et al.* 1997). All recovered neurones ($n = 10$) had morphological features typical of TC neurones of the cat VB thalamus (cf. Turner *et al.* 1997). The slightly larger inward rectification for Type II (compared to Type I) TC neurones reported in the accompanying paper (Turner *et al.* 1997) did not correspond to any difference in the properties of the currents investigated in this study, supporting the suggestion that it is simply a reflection of the larger apparent input resistance of Type II neurones (Turner *et al.* 1997). Drugs were obtained from the following sources: CNQX and APV, Tocris-Cookson; GYKI 52466, Research Biochemicals International; bicuculline methiodide, tetrodotoxin and tetraethylammonium chloride, Sigma; CGP 35348, MK 801 and ZD 7288 were kindly donated by Dr W. Froestl (Ciba-Geigy, Switzerland), Merk, Sharpe & Dolme (UK) and Dr P. Marshall (Zeneca, UK), respectively. Numerical results are expressed in the text as means ± S.E.M., and statistical significance was tested ($P = 5\%$) using Student's t test.

Computer simulations

A simplified model of a TC neurone was constructed using a single compartment incorporating the currents I_h and I_{KIR} of the Hodgkin–Huxley form. In addition, a K^+ leak current (I_{Leak}) was included. The equation describing the evolution of the membrane potential with time was:

$$C_m (dV/dt) = -(I_{Leak} + I_h + I_{KIR}) + I_{inj},$$

where E is the membrane potential; C_m (= 50 pF) is the membrane capacitance and I_{inj} is the injected current. Each of the non-inactivating currents, I_h and I_{KIR}, were modelled by

$$I_x = g_x m^a (V - E_x),$$

where g_x is the maximal conductance of the current I_x; m is the activation variable, and a is its (integer) exponent and is equal to 3 for I_h, and 1 or 3 for I_{KIR}; E_x is the reversal potential. The other equations for I_h were as described by Tóth & Crunelli (1992):

$$m_\infty = 1/(1 + \exp((V + 75)/5{\cdot}5)),$$

$$\tau_m = 120820/\exp(0{\cdot}061 \times V), \text{ for } V > -77{\cdot}5 \text{ mV},$$

$$\tau_m = 29{\cdot}54/\exp(-0{\cdot}046 \times V), \text{ for } V \leqslant -77{\cdot}5 \text{ mV},$$

where m_∞ represents the activation at steady state, and τ_m the corresponding time constant.

The other equations for I_{KIR} were as described by Nisenbaum & Wilson (1995):

$$m_\infty = 1/(1 + \exp((V - E_k - 15)/10)),$$

$$\tau_m = 1.$$

The equation used to describe I_{Leak} was:

$$I_{Leak} = g_{Leak}(V - E_{Leak}).$$

The following values were assumed for the maximal conductances and reversal potential: $g_{Leak} = 5$ nS, $g_h = 10$ nS, $E_h = -33$ mV; $g_{KIR} = 100$ nS and $E_K = -95$ mV (but note that E_K was systematically varied in some simulations). The system of differential equations was integrated using a slightly modified version of the 4th order Runge–Kutta method with a constant step size of 0·1 ms.

RESULTS

The electrophysiological properties of TC neurones of the cat VB thalamus ($n = 57$) reported in this study were similar to those described in the accompanying paper (Turner *et al.* 1997). In particular, the resting membrane potential was $-63{\cdot}5 \pm 1{\cdot}4$ mV ($n = 18$; range, −50 to −77 mV) and the steady-state input resistance (measured in the steep region of the V–I relationship) was $97{\cdot}5 \pm 9{\cdot}6$ MΩ ($n = 18$; range, 38–160 MΩ).

Fast and time-dependent anomalous rectification

Anomalous rectification was apparent from the non-linear structure of the third quadrant of the V–I and I–V relationships recorded under current- and voltage clamp conditions, respectively (Figs 1*A* and 3*A*). Under current clamp conditions voltage responses showed both fast and time-dependent rectification (Fig. 1*A*). Fast rectification was apparent as the peak amplitude of negative voltage responses did not increase in a linear manner with the amplitude of negative current steps (Fig. 1*A*). Time-dependent rectification was manifest as a slow depolarizing sag generated during the course of negative voltage deviations (Fig. 1*A*) (cf. Turner *et al.* 1997). Similarly, under voltage clamp conditions, fast rectification was apparent from the non-linear relationship between the amplitude of current responses and negative voltage steps, when measured immediately after the settling of capacitative artifacts (Fig. 3*A*), whilst time-dependent rectification was manifest as a slowly activating inward current generated during the course of negative voltage steps (Fig. 3*A*).

In order to separate fast and time-dependent anomalous rectification we applied ZD 7288, that is known to block I_f in cardiac cells and I_h in other central neurones (BoSmith *et al.* 1993; Harris & Constanti, 1995) and Cs^+, a 'classical' blocker of I_h (McCormick & Pape, 1990; Soltesz *et al.* 1991). The application of ZD 7288 (100 μM, $n = 12$ of 13 neurones; 300 μM, $n = 11$ of 12 neurones) did not influence fast rectification, but completely blocked the depolarizing sag apparent during the course of negative voltage deviations (Fig. 1*A* and *B*) and led to membrane hyperpolarization ($6{\cdot}8 \pm 0{\cdot}5$ mV; range, 6–10 mV; $n = 23$). Similarly, in neurones recorded under voltage clamp conditions the application of ZD 7288 (100 μM, $n = 7$; 300 μM, $n = 6$) led to a blockade of the slow inward current (Fig. 3*A*), but in the majority of neurones did not alter the magnitude of instantaneous inward current, so that instantaneous I–V relationships were non-linear. In two of thirteen neurones, however, ZD 7288 linearized the instantaneous I–V relationship (Fig. 3*C*). All these effects of ZD 7288 occurred after an exposure time of about 40 min, whilst other agents applied in the same experiment had equilibrium effects within 10 to 20 min. The action of ZD 7288 was not use dependent ($n = 3$) (not illustrated), and was irreversible, so that no time-dependent rectification was observed from TC neurones recorded in a brain slice even more than 8 h following a single exposure to ZD 7288.

The effectiveness of ZD 7288-induced blockade of the time-dependent rectification in all the neurones tested is demonstrated in the subtraction curves illustrated in the graphs of Figs 4 and 5, where the amplitudes of voltage (Fig. 4) and current (Fig. 5) responses have been measured at peak (Fig. 4) or instantaneous (Fig. 5) and designated steady-state points and subtracted (see Methods). Under control conditions, these procedures generated curves that first deviated from zero at membrane potentials between −60 and −75 mV and increased in amplitude as a function of membrane potential negativity (Figs 4*A* and 5*A*). In the presence of ZD 7288, however, the subtraction curves remained flat until the membrane potential became more negative than approximately −90 mV (Figs 4*B*, 4*C*, 5*B* and

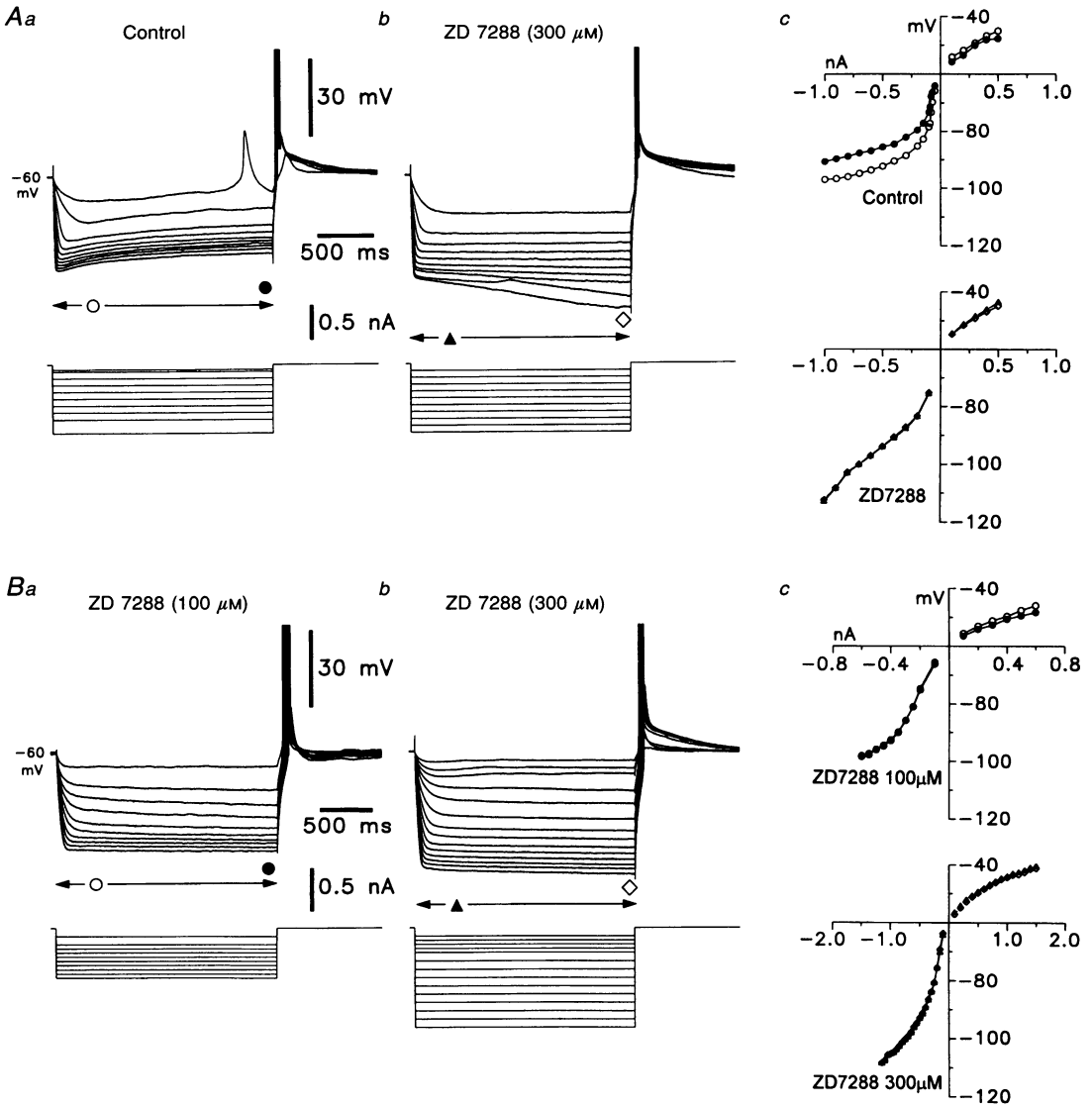

Figure 1. Fast and time-dependent anomalous rectification in TC neurones of the cat VB thalamus

A, superimposed families of negative voltage deviations (upper traces) evoked by negative current steps (lower traces). Control traces demonstrate the presence of a slow depolarizing sag apparent during the course of negative voltage deviations. A low-threshold Ca^{2+} potential is generated during the smallest voltage deviation in *a*. Addition of ZD 7288 (300 μM) to the perfusion medium led to a 10 mV hyperpolarization, and the control membrane potential was restored by DC injection. In the presence of ZD 7288 no depolarizing sag was apparent, but a slow hyperpolarizing ramp potential evoked in response to the largest negative current steps was revealed (*b*). The peak (open symbols) and steady-state (filled symbols) *V–I* relationships of this neurone are shown in *c*. *B*, ZD 7288 does not reveal the presence of a hyperpolarizing ramp potential in all TC neurones. The *V–I* relationship of two neurones exposed to ZD 7288 demonstrate inward and outward rectification (*c*), but no depolarizing sag or ramp hyperpolarization during the course of large negative voltage deviations. The amplitude of action potentials has been truncated for clarity.

5*C*). Note that under current clamp conditions the abrupt peaks in some subtraction curves ($n = 5$) at potentials between −65 and −75 mV represent the measurement of one or more low-threshold Ca^{2+} potentials generated during the course of negative voltage deviations.

The slow inward current ($n = 3$) (cf. Fig. 9) and the depolarizing sag apparent during the course of negative voltage excursions ($n = 6$) (not illustrated) were blocked by the application of Cs^{+} (3 mM). The effects of this agent upon the degree of fast rectification were, however, variable (not

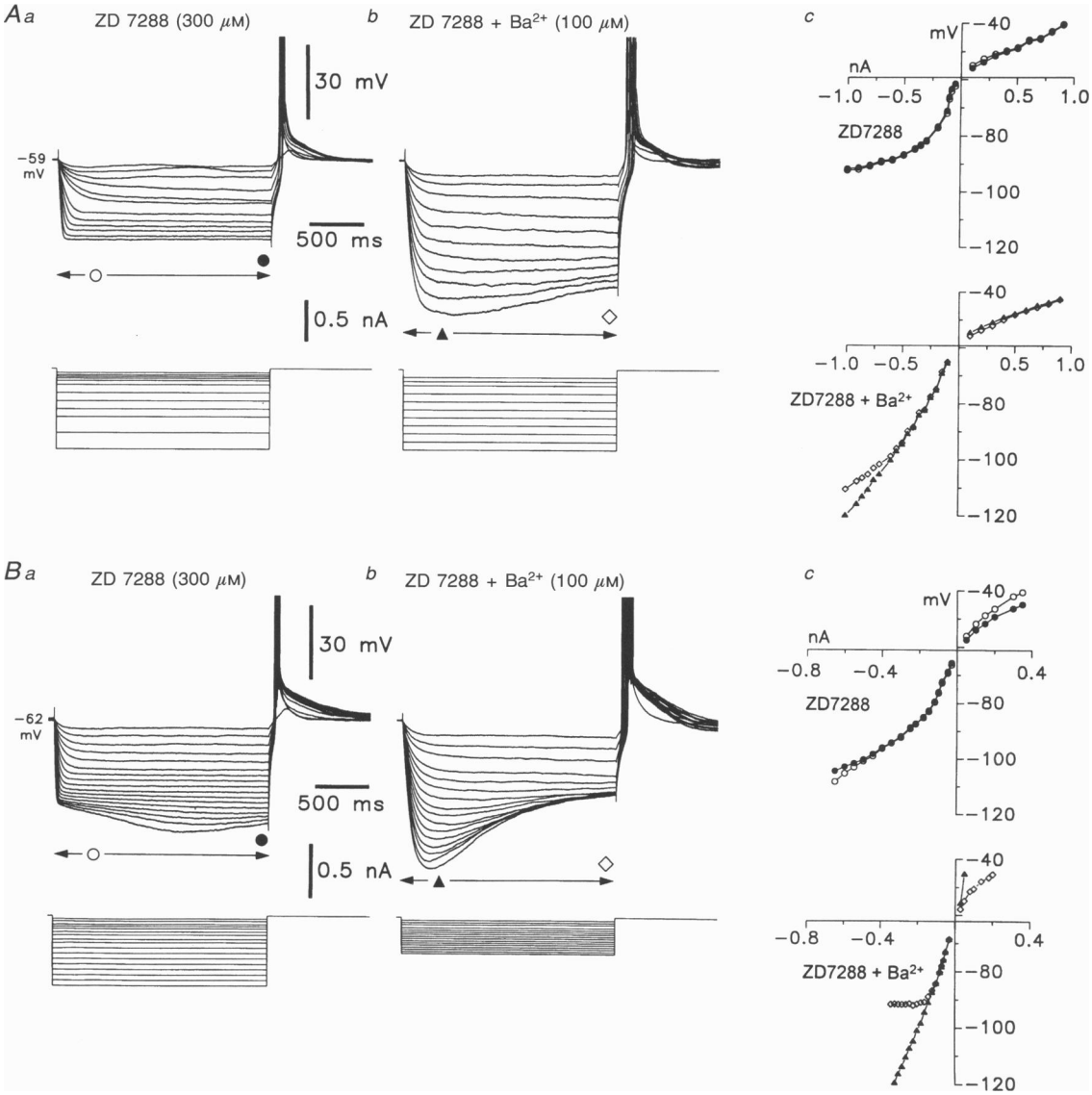

Figure 2. The pattern of anomalous rectification was transformed by Ba^{2+}

A, the *V–I* relationship of a neurone recorded in the presence of ZD 7288 (300 μM) shows no time-dependent rectification (*a*). The co-application of ZD 7288 and Ba^{2+} (100 μM) (*b*) increased the input resistance of the neurone and revealed the presence of a slow depolarizing sag potential that has a time course different from, and is first activated at potentials about 20 mV more negative than, the sag present under control conditions (cf. Fig. 1*Aa*). The peak (open symbols) and steady-state (filled symbols) *V–I* relationships (*c*) constructed in the presence of ZD 7288 alone and in the presence of ZD 7288 and Ba^{2+} are distinct, and indicate that in the presence of Ba^{2+} the peak amplitude of negative voltage deviations is linearly related to the magnitude of the current step. *B*, the voltage deviations in response to negative current steps in a different neurone, recorded in the presence of ZD 7288 (300 μM) alone, demonstrates a complex charging pattern, characterized by a time-dependent increase in input resistance: this effect is truncated by a slow depolarizing sag potential (*a* and *b*). The co-application of ZD 7288 and Ba^{2+} (100 μM) blocked the complex charging pattern and revealed the presence of a large amplitude depolarizing sag (*b*). The *V–I* relationships of this neurone demonstrate that ZD 7288 and Ba^{2+} (*c*) linearizes the *V–I* relationship when measured at the peak of voltage deviation, and reveals the magnitude of inward, time-dependent rectification (cf. Fig. 1*Ac* and *Bc*). The amplitude of action potentials has been truncated for clarity.

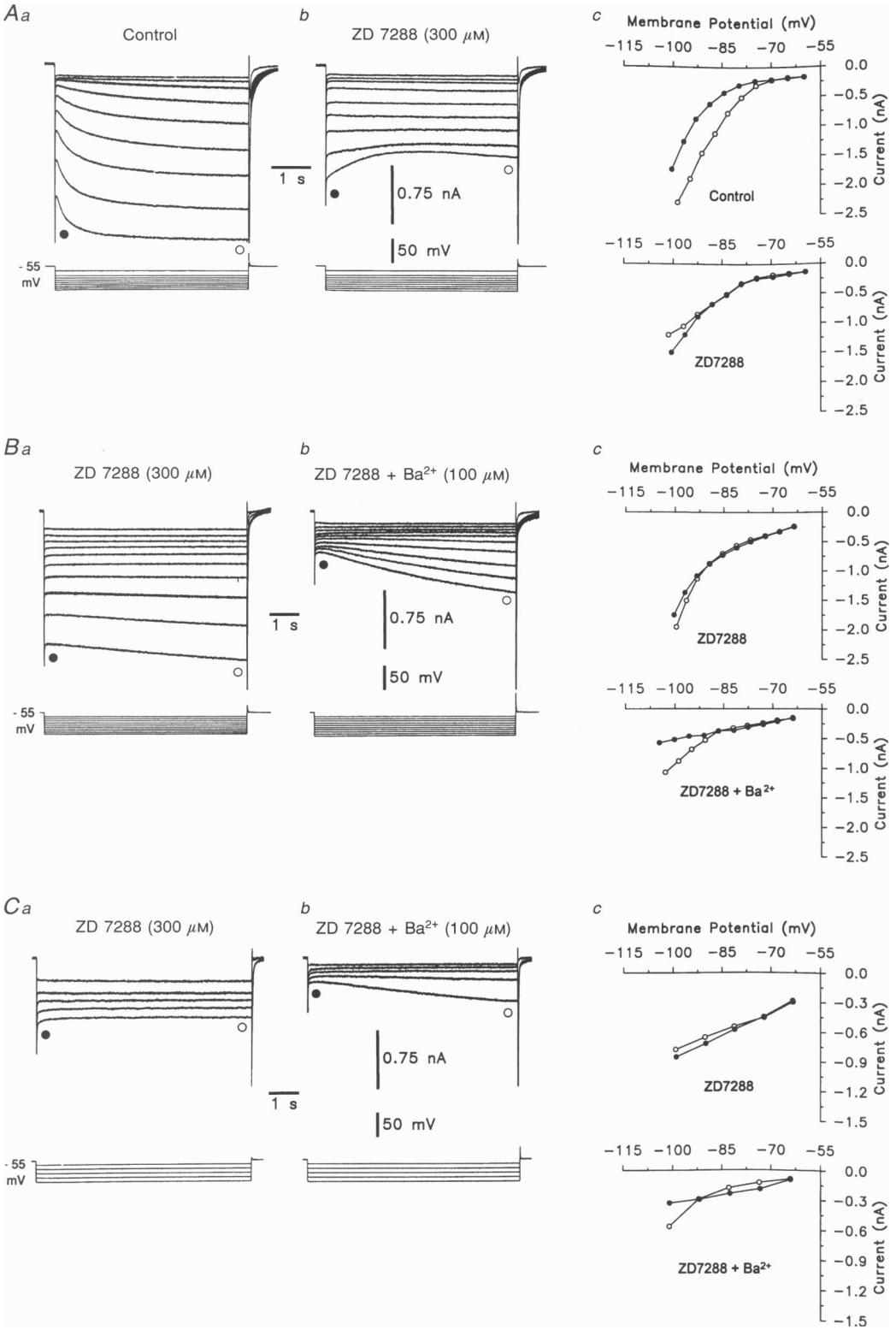

Figure 3. Rectification properties of TC neurones of the VB thalamus recorded under voltage clamp in different experimental conditions

A, superimposed families of membrane current (upper traces) and voltage command steps (lower traces). A slow inward current was generated during the course of negative voltage steps of amplitude greater than 10 mV (*a*). Note that an instantaneous inward current was concurrently activated. The bath application of ZD 7288 (300 μM) abolished the slow inward current, but did not block the fast inward current (*b*). In the presence of ZD 7288 a fading of the instantaneous inward current was followed by the activation of a very slow inward current during the course of large negative voltage commands. Under control conditions, the

illustrated) limiting the use of Cs^+ for an analysis of fast rectification. By comparison with previous recordings of TC neurones, we suggest that the slow inward current and the depolarizing sag potential represent the activation of the hyperpolarization-activated current (I_h, McCormick & Pape, 1990; Soltesz *et al.* 1991). Our results, therefore, demonstrate that ZD 7288 blocks I_h but does not influence the degree of fast rectification, indicating that fast rectification is not formed by I_h.

Together with the blockade of I_h, in other neurones ($n = 5$) the application of ZD 7288 led to the appearance of voltage responses that were characterized by a time-dependent increase in input resistance, that was only apparent for hyperpolarizing voltage responses of amplitude greater than 30 mV (Fig. 1*Ab*). This time-dependent increase in input resistance was reflected under voltage clamp conditions as a fading of the instantaneous inward current elicited by large amplitude (> 30 mV) voltage commands (Fig. 3*Ab*) ($n = 3$). Finally, in yet another group of neurones the generation of a sag potential ($n = 2$) (not illustrated) or a slow inward current ($n = 4$) apparent at membrane potentials more negative than −90 mV and with very slow activation kinetics was noted (Fig. 3*Ba*). These data indicate that TC neurones exhibit time-dependent ionic mechansims other than I_h.

Fast anomalous rectification in other central neurones has been suggested to be mediated by an inwardly rectifying K^+ current (I_{KIR}) (Constanti & Galvan, 1983; Uchimura *et al.* 1989; Sutor & Hablitz, 1993; Womble & Moises, 1993; Nisenbaum & Wilson, 1995). Since the 'classical' form of I_{KIR} allows appreciable current flow only at membrane potentials more negative than E_K (Hagiwara *et al.* 1976, 1978; Gay & Stanfield, 1977; Standen & Stanfield, 1978), we investigated the voltage at which fast rectification was first apparent in TC neurones where I_h had been blocked by ZD 7288 (100 μM, $n = 12$; 300 μM, $n = 11$). Analysis of the peak *V–I* relationships of these neurones showed that rectification was clearly apparent from membrane potentials more negative than −80 mV (cf. Figs 1 and 2). Although E_K could not be accurately calculated in our study, an E_K value of approximately −95 mV has been indicated for TC neurones recorded under conditions identical to the ones used in the present study (Crunelli, Haby, Jassik-Gerschenfeld, Leresche & Pirchio, 1988; Williams, Turner & Crunelli, 1995). These data therefore indicate that fast rectification may first be apparent at membrane potentials more positive than E_K. To test the involvement of I_{KIR} in the formation of fast rectification we applied the I_{KIR} blocker Ba^{2+} at a low concentration (100 μM) in order to reduce the non-selective blockade of other K^+ currents, in the continuous presence of ZD 7288. In each neurone tested ($n = 8$) Ba^{2+} (100 μM) linearized peak third quadrant *V–I* (Fig. 2*A* and *B*) and instantaneous *I–V* relationships (Fig. 3*B* and *C*) and led to a membrane depolarization (13·3 ± 4·2 mV; control, −72·0 ± 3·0 mV; range, −64 to −85 mV; Ba^{2+}, −58·7 ± 2·5 mV; range, −50 to −71 mV) or the appearance of a tonic inward current (192 ± 36 pA; range, 120–280 pA). The steady-state input resistance was not significantly altered by Ba^{2+} (control, 90·9 ± 12·6 MΩ; range, 44·3–144·2 MΩ; Ba^{2+}, 139·1 ± 33·4 MΩ; range, 79·2–297·9 MΩ; $t = 1·47$). It is important to note that in three (of 8) neurones, a time-dependent increase in input resistance was noted, where large amplitude (> −30 mV) voltage responses possessed a pronounced inflection in the charging pattern evoked at the onset of negative current steps (not illustrated). This time-dependent increase in input resistance observed in the presence of Ba^{2+} was similar in structure to that expressed by some neurones recorded in the presence of ZD 7288 alone (cf. Fig. 1*A*), and was mirrored under voltage clamp conditions as a fading of the instantaneous inward current (not illustrated).

The very slow activating inward current, $I_{h,slow}$

The most striking effect of Ba^{2+} applied in the continous presence of ZD 7288, however, was the presence of a very slow depolarizing sag, apparent during the course of large (> 30 mV) negative voltage deviations (Fig. 2*A* and *B*). These depolarizing sag potentials had slower activation kinetics and a different voltage dependence from those observed under control conditions (compare Fig. 1*A* with Fig. 2*B*). Under voltage clamp conditions, these very slow depolarizing sags were reflected by the generation of a very slow inward current that was first activated from a membrane potential of about −90 mV (Fig. 3*B* and *C*). It should be noted that this current was activated in neurones that either demonstrated linear or non-linear *I–V* relationships when recorded in the presence of ZD 7288

instantaneous (filled symbols) and steady-state (open symbols) *I–V* relationships were non-linear and quite distinct, indicating the presence of a slow inward current (*c*). In the presence of ZD 7288 instantaneous and steady-state curves were identical over a potential range between −60 to −90 mV. *B*, the *I–V* relationship of another TC neurone exposed to ZD 7288 (300 μM) demonstrated fast rectification. Note that during the course of large negative voltage steps a very slow activating inward current was apparent (*a* and *c*). The co-application of ZD 7288 and Ba^{2+} (100 μM) reduced the fast inward current (*b*) and linearized the instantaneous *I–V* relationship (*c*). Ba^{2+}, however, led to the appearance of an inward current with very slow activation kinetics, activated at membrane potentials more negative than −85 mV. *C*, the *I–V* relationship of a different neurone recorded in the presence of ZD 7288 (300 μM) showed no evidence for a very slow inward current (*a* and *c*). The co-application of ZD 7288 and Ba^{2+} (100 μM) led to a reduction of the input conductance of the neurone and the appearance of an inward current with very slow activation kinetics at potentials more negative than −85 mV (*b* and *c*). The amplitude of the low-threshold Ca^{2+} current activated following the offset of negative voltage steps has been truncated for clarity.

alone, so that this form of current may arise *de novo* following the application of Ba^{2+} (Fig. 3*C*). The subtraction curves shown in Fig. 4*D* illustrate that the application of Ba^{2+} led to the generation of a depolarizing sag with an amplitude far greater than, and a voltage dependence quite different from, that observed in control neurones (Fig. 4*A*). This was reflected by the presence of an inward current with an activation threshold about 20 mV more negative than that of I_h (Fig. 5*D*). As this current was activated by membrane hyperpolarization and had very slow activation kinetics we refer to it as $I_{h,slow}$. A representative example of $I_{h,slow}$ is illustrated in Fig. 6, where it may be seen that this current is first activated at potentials more negative than −90 mV and reaches a steady value after 25 s. We suggest that this is true inward current, as the input conductance of the neurone was found to increase during the course of current activation (Fig. 6*B*). Therefore, plots of apparent input conductance against voltage allowed estimates of the activation threshold and range of the slow inward current (Fig. 6*A*). A full activation curve of $I_{h,slow}$, however, could

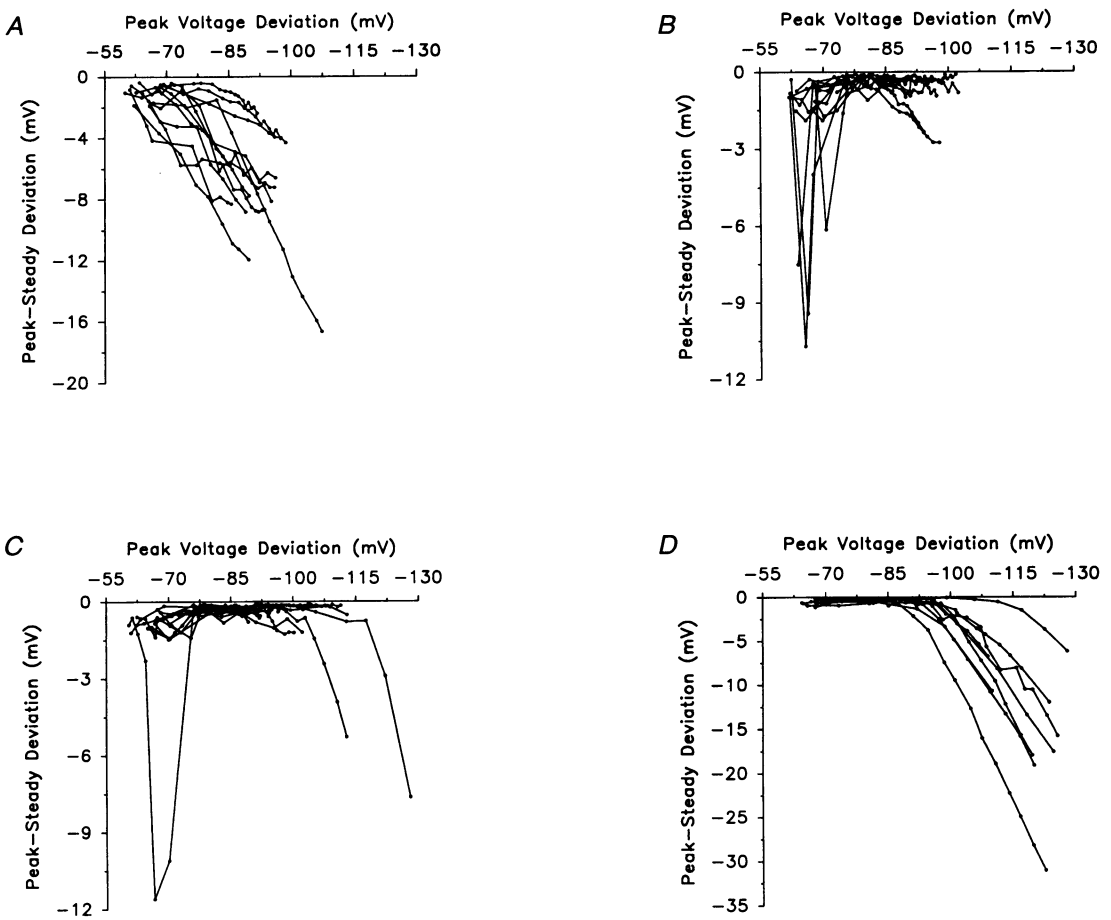

Figure 4. The structure of time-dependent rectification recorded under current clamp conditions in TC neurones during different experimental conditions

A, under control conditions the subtraction of the amplitudes of negative voltage deviations evoked by negative current steps, when measured at their negative peaks and steady-state points, revealed a curve that first deviated from zero in a range between −55 and −70 mV. The amplitude of the curve increased as a function of membrane potential negativity, which is measured at the negative peak of voltage deviations. *B*, the application of ZD 7288 (100 μM) revealed a different pattern of rectification: in the majority of neurones the voltage curve did not deviate from zero, whilst the results of two neurones were similar to control. The abrupt peaks apparent between −60 to −75 mV in the curves produced in some neurones were formed by the measurement of low-threshold Ca^{2+} potentials generated at the designated steady-state time. *C*, the curves produced in neurones exposed to ZD 7288 (300 μM), were similar to those exposed to 100 μM, but note the representation of a slow sag potential in two neurones, generated at potentials more negative than −100 mV. *D*, in neurones exposed to the co-application of ZD 7288 (100–300 μM) and Ba^{2+} (100 μM), the subtraction voltage curve did not deviate from zero until peak voltage deviations were more negative than −90 mV, and then increased as a linear function of membrane potential negativity, reflecting the generation of a slow depolarizing sag.

not be constructed as reasonable voltage control was lost at potentials more negative than about −130 mV, where the amplitude of $I_{h,slow}$ was still increasing. Conductance plots gave similar results to those of subtraction curves of instantaneous and steady-state current, and showed that $I_{h,slow}$ first activated at potentials between −85 and −90 mV and increased linearly in magnitude with increasing membrane potential negativity (Fig. 6*A*).

The activation of $I_{h,slow}$ may have been a product of Ba^{2+}-induced modification of I_h following blockade by ZD 7288. To test this possiblity we applied Ba^{2+} to control neurones (Fig. 7) ($n = 3$). Ba^{2+} (0·1–2 mM) led to a tonic inward current and linearized instantaneous *I–V* relationship, indicating that instantaneous *I–V* relationship, under control conditions, are Ba^{2+} sensitive, whilst the activation range, kinetics and amplitude of I_h were not largely affected (Fig. 7). Under such conditions, the addition of ZD 7288 (300–500 μM) led to a blockade of I_h and revealed the activation of $I_{h,slow}$ (Fig. 7*A* and *C*).

In order to distinguish further $I_{h,slow}$ from I_h we approximated the activation kinetics of these currents by the fitting of mono- or bi-exponential functions to current traces (Fig. 8). The activation kinetics of I_h was best approximated by a bi-exponential fit (Fig. 8*A* and *C*), and

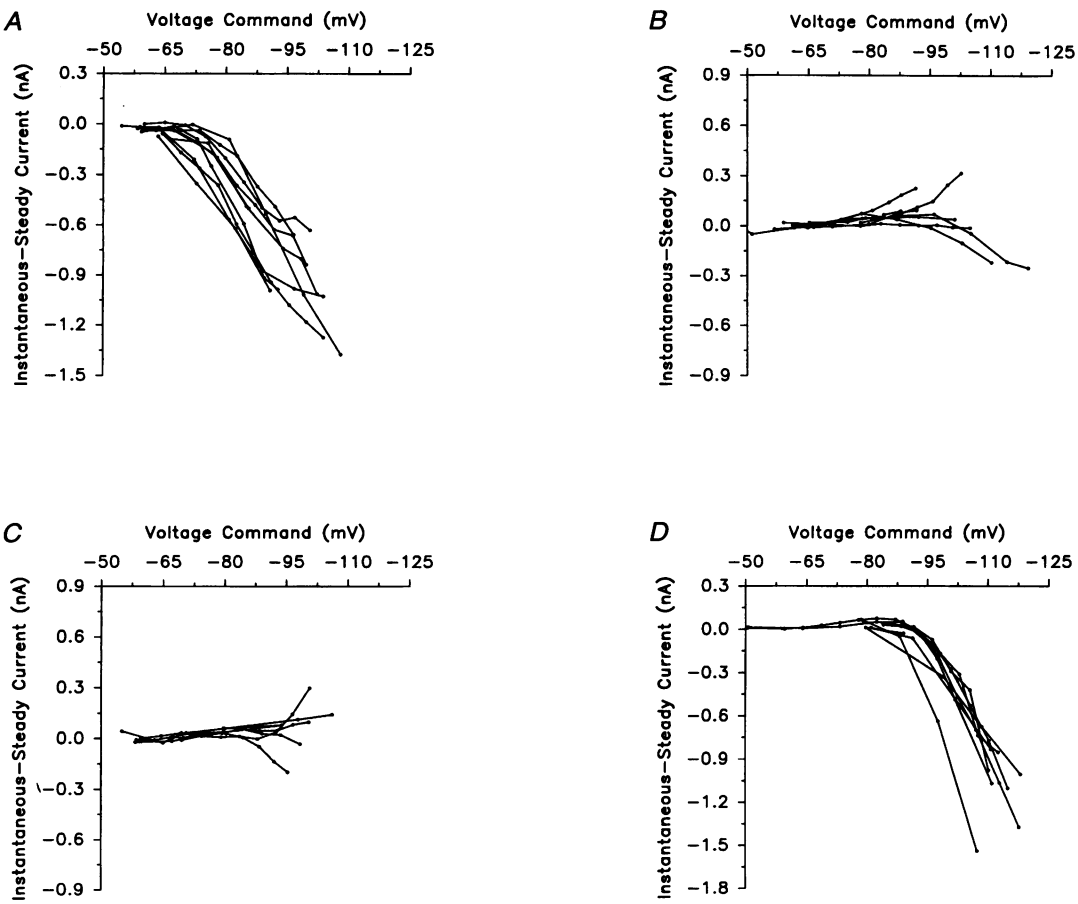

Figure 5. The structure of time-dependent anomalous rectification recorded under voltage clamp in TC neurones during different experimental conditions

A, the *I–V* relationship in the hyperpolarized direction under control conditions is dominated by the slow activation of an inward current. The subtraction of *I–V* relationships formed at instantaneous and steady-state points (see Methods) produced a curve that first deviated from zero in the inward direction at membrane potentials between −60 and −70 mV, and increased in amplitude as a linear function of membrane potential negativity. *B*, in the presence of ZD 7288 (100 μM) all but one of the subtraction curves did not deviate from zero until potentials were more negative than −90 mV. At this potential both outward and inward subtraction curves were apparent. *C*, subtraction curves produced in the presence of ZD 7288 (300 μM) were linear and centred around zero over a potential range of −55 to −85 mV. At membrane potentials more negative than these values, inward or outward deviations were apparent. *D*, in the presence of ZD 7288 (100–300 μM) and Ba^{2+} (100 μM), subtraction curves significantly deviated from zero at membrane potentials between −85 to −90 mV, and increased in amplitude as a roughly linear function of membrane potential negativity.

was slowest at potentials where the current first activated, becoming then relatively faster as a function of membrane negativity. Such analysis revealed the time constants τ_{fast} and τ_{slow} to be broadly voltage dependent. However, in some neurones τ_{slow} was found first to decrease and then increase with membrane potential negativity (Fig. 8*C*), indicating either unreliable voltage clamp, or that a current with slow activation kinetics (such as $I_{h,slow}$) was activated at membrane potentials more negative than −90 mV and contributed to the net current flow under control conditions. The activation kinetics of $I_{h,slow}$ were found to be much slower than those of I_h (Fig. 8*B* and *D*) and, in contrast to the results obtained with I_h, τ_{fast} was weakly related to membrane potential negativity. It may be argued, therefore, that τ_{fast} is not a function of membrane voltage, but rather reflects contamination by capacative artifacts. Nevertheless, either τ_{slow} or the mono-exponential τ of $I_{h,slow}$ were found to be in all cases two- to threefold slower than the corresponding time constants used to describe I_h (compare Fig. 8*C* with 8*D*).

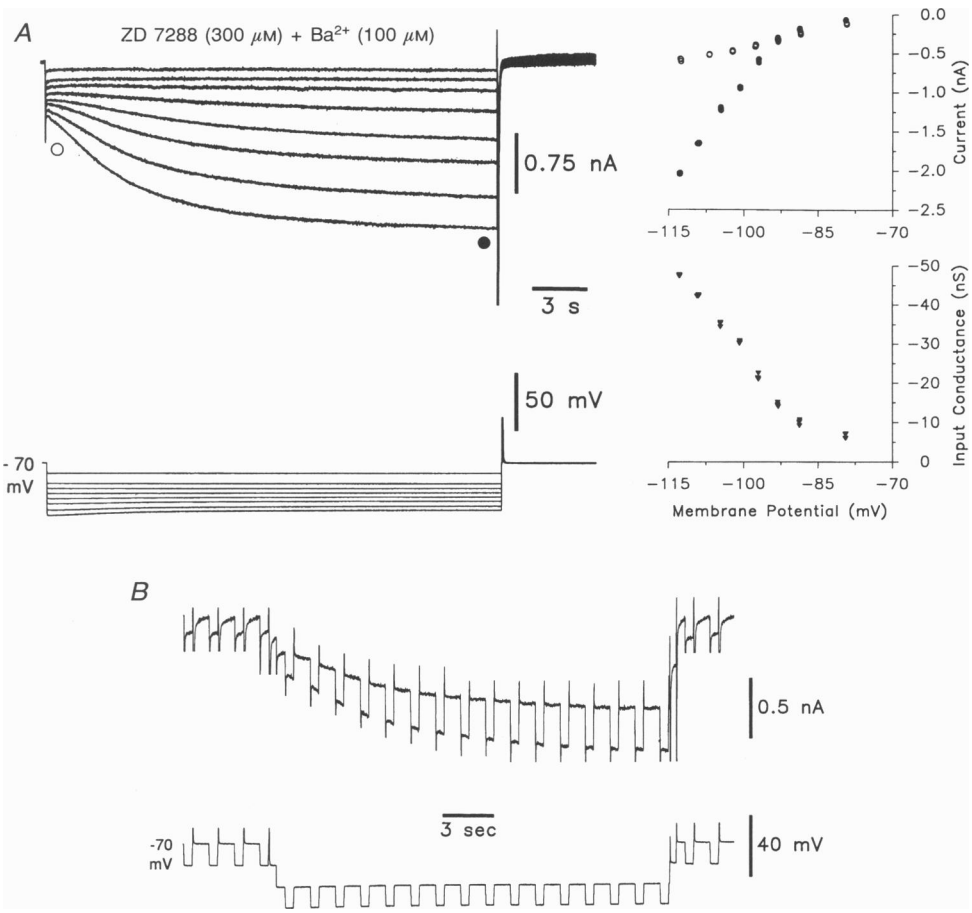

Figure 6. $I_{h,slow}$ was associated with an increase in membrane conductance

A, superimposed families of membrane currents (upper records) and voltage commands (lower records) recorded in the presence of ZD 7288 (300 μM) and Ba^{2+} (100 μM). $I_{h,slow}$ was first activated during the course of voltage commands to −93 mV, and its kinetics of activation were voltage dependent. The instantaneous current–voltage relationship (open symbols) was linear across the entire voltage range tested, whilst the steady-state relationship was non-linear (filled symbols). The four consecutive current traces recorded for each voltage step were similar, indicating the reproducibilty of the membrane current. The inward current was associated with an increase in input conductance, and once the slow inward current was activated the increase in input conductance was a linear function of membrane potential negativity (lower graph). *B*, the slow inward current is associated with an increase in input conductance (records from the same neurone as in *A*). Small negative voltage steps were used to gauge the neurones input conductance before, during and following a long negative voltage step. The evolution of the inward current was parallelled by a rise in input conductance. Note, that at the offset of the large negative voltage deviation a small increase in input conductance was apparent, which was associated with the deactivation of the slow inward current. The amplitude of the low-threshold Ca^{2+} current has been truncated for clarity.

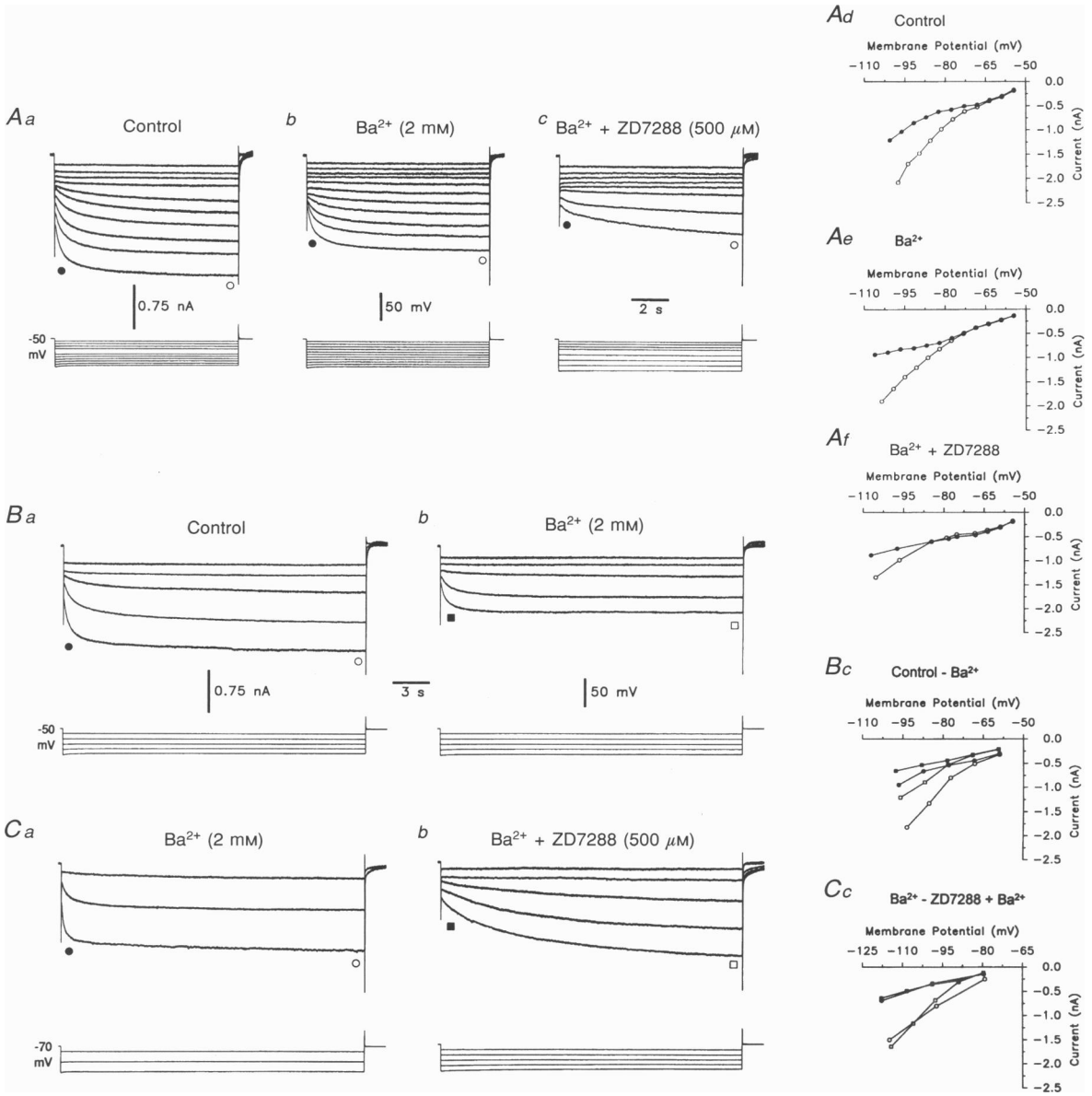

Figure 7. The application of Ba^{2+} did not alter the activation properties of I_h

A, families of membrane currents (upper traces) and voltage commands (lower traces) show that the application of Ba^{2+} reduced the instantaneous inward current, but did not affect the properties of I_h. The co-application of Ba^{2+} and ZD 7288, however, resulted in a blockade of I_h, whilst revealing the presence of $I_{h,slow}$. The instantaneous and steady-state *I–V* relationships are non-linear under control conditions (*Ad*). The application of Ba^{2+} linearized the instantaneous *I–V* relationship (*Ae*), but did not alter the steady-state relationship, whilst in the presence of Ba^{2+} and ZD 7288 instantaneous (filled symbols) and steady-state (open symbols) relationships did not diverge until the membrane potential was stepped to values more negative than −90 mV (*Af*). *B*, Ba^{2+} does not alter the form of I_h when evoked for a period of 25 s from a holding potential of −50 mV. *Bc* shows the instantaneous (filled symbols) and steady-state (open symbols) *I–V* relationships in control conditions (circles) and in the presence of Ba^{2+} (squares). *C*, the co-application of Ba^{2+} and ZD 7288, however, blocked I_h and led to the appearance of $I_{h,slow}$. In this neurone a direct comparison between the activation characteristics of I_h and $I_{h,slow}$ can be made, and it indicates that these currents are distinct in terms of kinetics and voltage dependence. *Cc* shows the instantaneous and steady-state *I–V* relationships in the presence of Ba^{2+} (circles) and during co-application of Ba^{2+} and ZD 7288 (squares). The amplitude of the low-threshold Ca^{2+} current has been truncated for clarity.

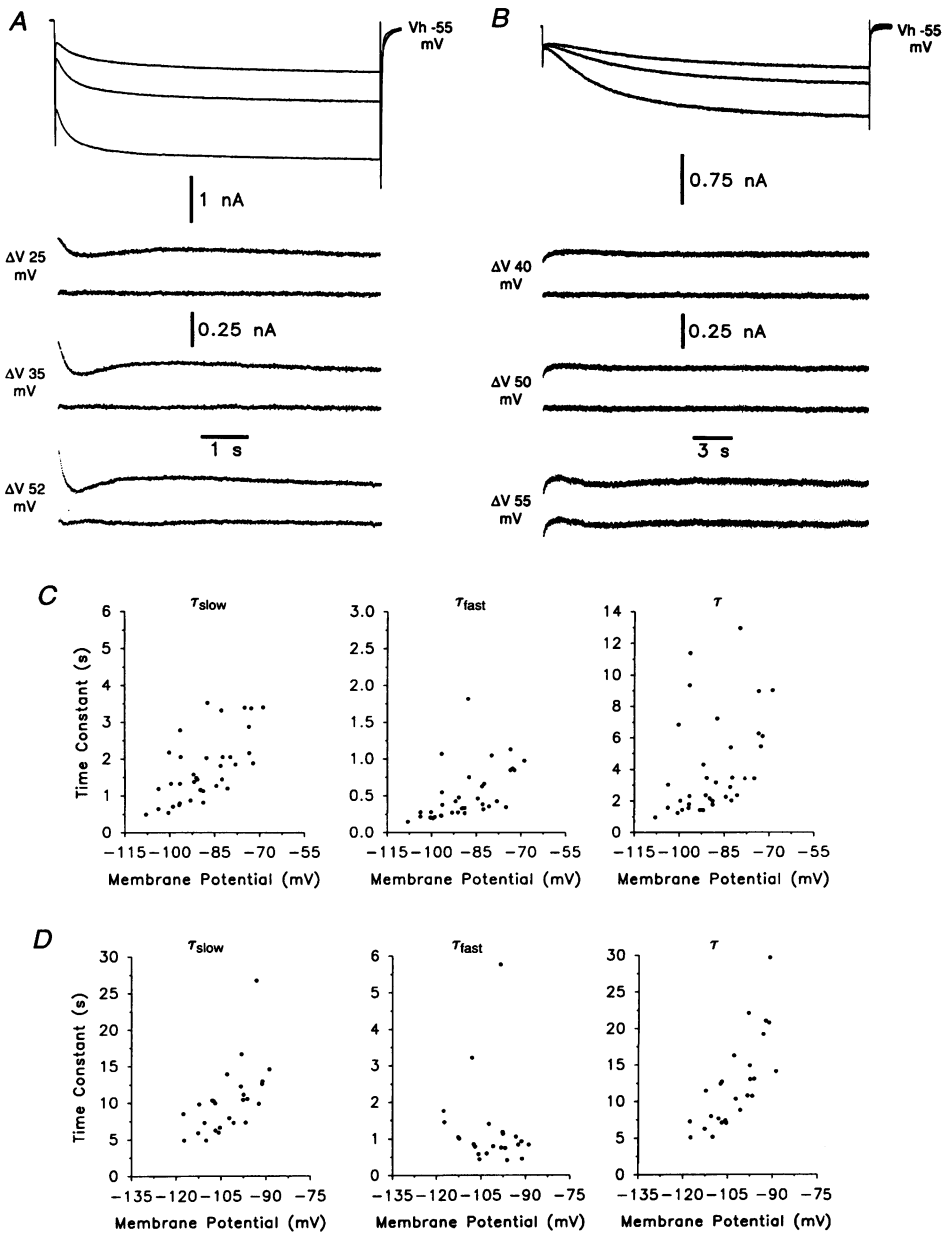

Figure 8. The activation kinetics of I_h and $I_{h,slow}$ were different

A, a representative example of the kinetic analysis of I_h. Current records were approximated with a single or the sum of two exponential functions. The digital subtraction of the current records and exponential functions are shown below the three superimposed current records. For each of these current records the residuals from a single exponential (upper trace) or from the sum of two exponential functions (lower trace) are illustrated (ΔV indicates the amplitude of the voltage commands). Note that for each current record the sum of two exponential functions produced a closer approximation. *B*, an example of similar analyses for a representative example of $I_{h,slow}$. For this current the sum of two exponential functions also best approximated the current records. Note, however, that the approximation was not as good for the current of largest amplitude ($\Delta V = 55$ mV). *C*, the time constants of the exponential functions used to approximate I_h are plotted against membrane potential. The time constants of the two exponential functions (τ_{slow} and τ_{fast}) and the time constant of the single exponential function (τ), are illustrated from left to right, respectively. Note, that the values of τ and τ_{slow} are not uniform functions of membrane potential, as relatively slow terms are apparent at very negative membrane potentials. *D*, the time constants of the exponential functions used to approximate $I_{h,slow}$ are plotted against membrane potential. The time constants τ and τ_{slow} for $I_{h,slow}$ are related to membrane potential. These time constants were slower at potentials where the current was first activated and relatively faster at more negative membrane potentials. No obvious relationship between τ_{fast} and membrane potential, however, was apparent.

The ionic basis of $I_{h,slow}$ was studied by an anaysis of its reversal potential and by the use of pharmacological blockers. By comparison with the results of others, we reasoned that $I_{h,slow}$ may represent the activation of a neuronal form of the inwardly rectifying Cl^- current I_{ClC2} (Staley, 1994). Zn^{2+} (200 μM) ($n = 2$), a blocker of I_{ClC2}, however, did not alter the amplitude or voltage dependence of $I_{h,slow}$ (not illustrated), and recordings made with microelectrodes filled with 3 M potassium chloride, a procedure shown to alter the equilibrium potential of chloride (E_{Cl}) in TC neurones (Crunelli *et al.* 1988), did not have any effects on $I_{h,slow}$ (Fig. 10), suggesting that $I_{h,slow}$ does not represent I_{ClC2}. High concentrations of Cs^+ (5 mM), however, produced a greater than 90% reduction in the amplitude of $I_{h,slow}$ (93 ± 2·3%, $n = 4$) (Fig. 9). In addition to reducing the amplitude of $I_{h,slow}$, Cs^+ led to a reduction in neuronal input conductance, possibly by an action on the leak conductance (Fig. 9) (Constanti & Galvan, 1983; Soltesz *et al.* 1991). We estimated the potential at which the tail current of $I_{h,slow}$ reversed (Fig. 10), under conditions where pure Na^+ and K^+ currents were blocked with tetrodotoxin (1 μM) and reduced by tetraethylammonium chloride (10 mM), respectively. Such analysis was, however, complicated by the presence of I_T (Crunelli, Lightowler & Pollard, 1989) generated at the offset of the long (> 15 s) negative voltage steps used to evoke $I_{h,slow}$, even when the perfusion medium contained low Ca^{2+} (0·5 mM), high Mg^{2+} (12 mM) and Ni^{2+} (3 mM) (cf. Crunelli *et al.* 1989) (Fig. 10). Despite this, the slow nature of $I_{h,slow}$ tail currents allowed an approximation of their reversal potential, which was found to lie between −65·3 ± 3·8 and −56·6 ± 4·0 mV ($n = 3$) when recorded with potassium acetate electrodes, and between −57·6 ± 3·8 and −50·3 ± 3·2 mV ($n = 3$) when recorded with potassium chloride electrodes.

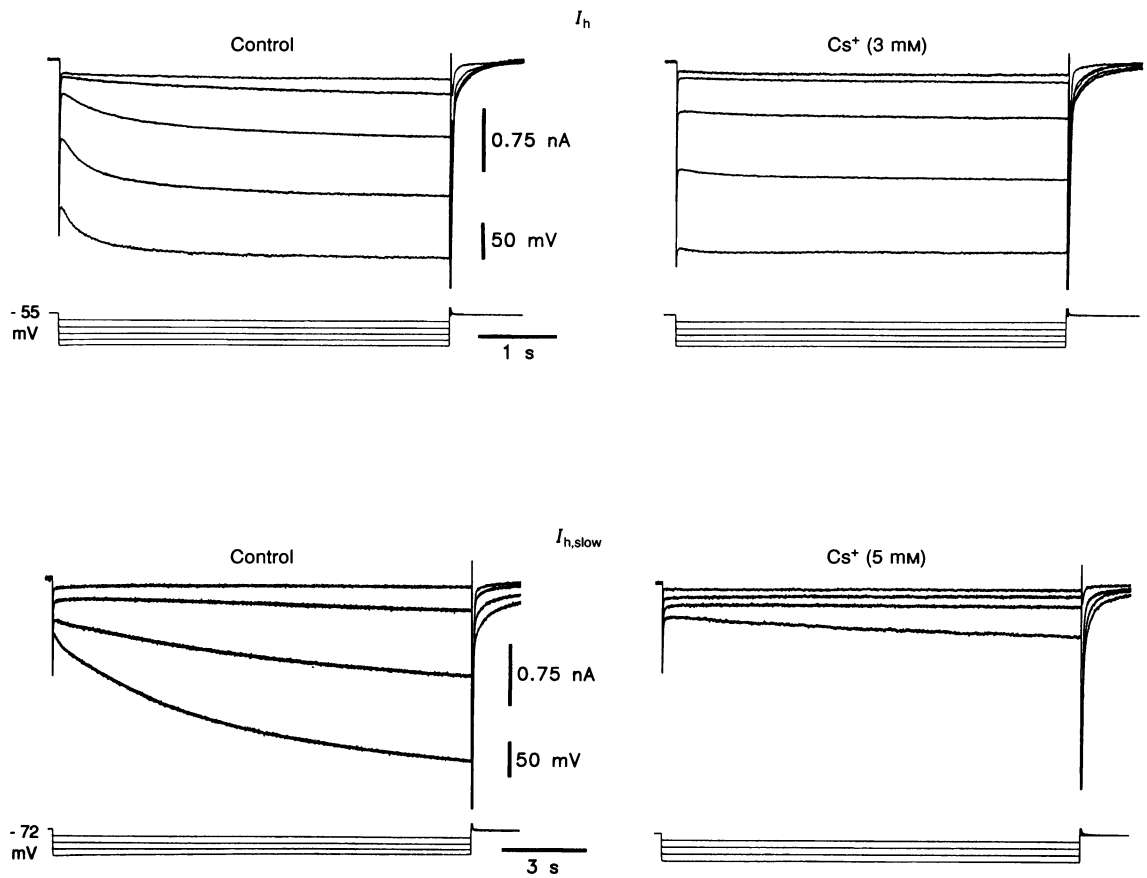

Figure 9. $I_{h,slow}$ and I_h had a different sensitivity to Cs^+

The upper panel demonstrates superimposed families of current (upper traces) and voltage (lower traces) records, under control conditions and following the application of Cs^+ (3 mM). Note that Cs^+ blocked I_h, but that fast anomalous rectification was not effected at this concentration of Cs^+. The lower panel demonstrates that $I_{h,slow}$ was greatly reduced by the application of Cs^+ (5 mM). Superimposed families of membrane current (upper traces) and voltage command steps (lower traces) recorded under control conditions, i.e. in the presence of ZD 7288 (300 μM) and Ba^{2+} (2 mM) show the activation of $I_{h,slow}$. The application of Cs^+ reduced both this current and the input conductance of the neurone. Note the different time calibration of the upper and lower sets of records, and that the amplitude of the low-threshold Ca^{2+} current has been truncated for clarity.

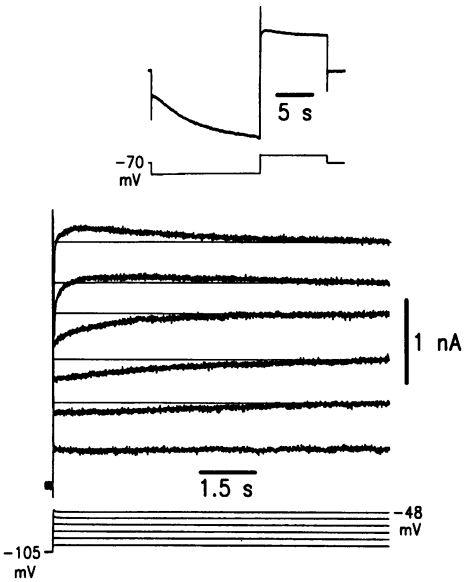

Figure 10. The reversal potential of $I_{h,slow}$ tail currents
The voltage protocol and form of current used to estimate the reversal potential of $I_{h,slow}$ is shown in the inset. For experiments of this kind, the content of the extracellular environment was selected so as to reduce the amplitude of the low-threshold Ca^{2+} current, I_T, and other membrane currents activated at membrane potentials more positive than −60 mV (see text). The tail currents of $I_{h,slow}$ are initially superimposed upon a residual I_T. The slow deactivation kinetics of $I_{h,slow}$, however, allowed an estimate of their reversal potential. The neurone was recorded with an electrode filled with 3 M potassium chloride.

In substantia nigra neurones, Harris & Constanti (1995) have suggested that the blockade of I_h by ZD 7288 may be relieved by intense membrane hyperpolarization (more negative than −90 mV), so that during the course of large negative voltage steps of long duration (> 30 s) a slow inward current becomes apparent. We tested the possibility that $I_{h,slow}$ may represent the voltage-dependent relief of the ZD 7288 blockade of I_h by measuring the input conductance of neurones before and after a period of maintained negativity (more negative than −95 mV) ($n = 3$).

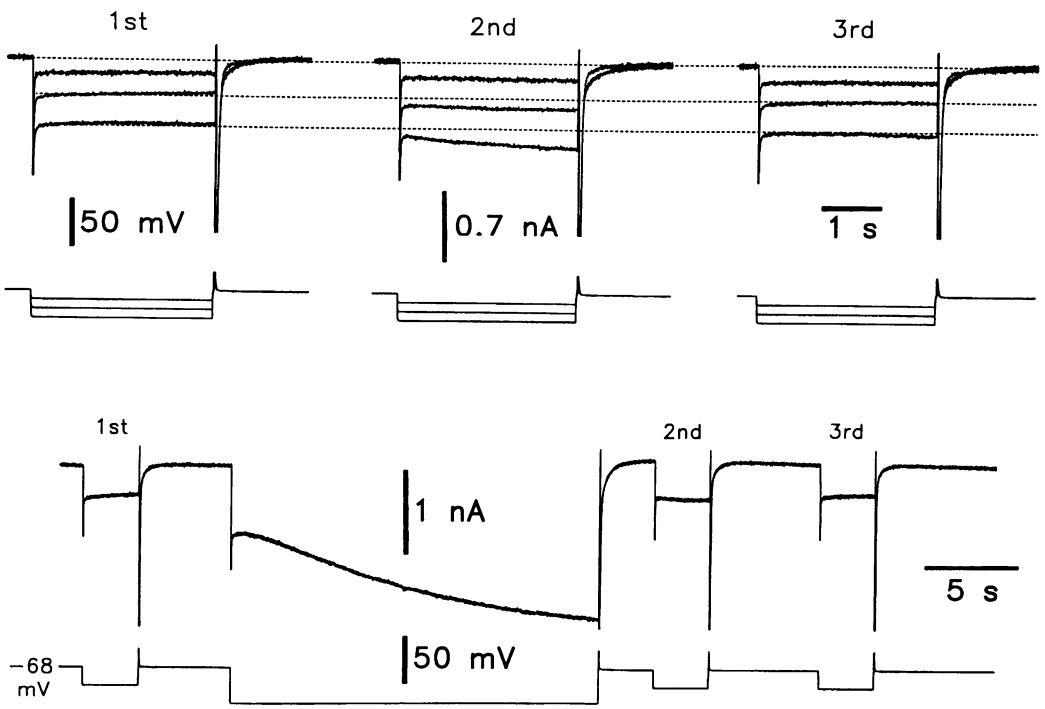

Figure 11. $I_{h,slow}$ is not a product of a relief of I_h blockade
The lower continuous records demonstrate the experimental protocol, where relatively short voltage steps were applied before (1st) and after (2nd and 3rd) a large and long voltage step. The currents produced by the short voltage steps are shown at a faster time base at the top of the figure. Three current responses (upper traces) generated by three different voltage steps (lower traces) have been superimposed and are offset to allow a direct comparison of the apparent input conductance between the 1st, 2nd and 3rd responses. A small increase in apparent conductance is apparent following the offset of the long voltage step (2nd); in response to the largest short voltage step a time-dependent inward current is apparent, that represents current flow through open $I_{h,slow}$ channels. This TC neurone was recorded in the presence of ZD 7288 (300 μM) and Ba^{2+} (100 μM).

As shown in Fig. 11, a small and transient voltage-dependent increase in input conductance is apparent at the offset of a long negative voltage step. The transient nature and small amplitude of this increase in input conductance suggests that it is formed by the deactivation of $I_{h,slow}$ and does not represent a voltage-dependent relief of ZD 7288 blockade of I_h, since the voltage range over which the input conductance of the neurone was increased is completely different to that of I_h. Furthermore, we have no *a priori* reason to suggest that the kinetics of the relief of I_h blockade by ZD 7288 will be different to those of blockade. Indeed, this is not the case as the input conductance returned to control values within 10 to 15 s following the offset of a large negative voltage pulse, whilst steady-state activation of $I_{h,slow}$ required at least 25 s.

Computer simulations

We investigated the involvement of the voltage-activated currents I_{KIR} and I_h and of the leak K^+ current, I_{Leak} in the formation of anomalous rectification with computer simulations. It was not our intention to simulate the kinetic properties of active conductances accurately, thus I_{KIR} was modelled according to Nisenbaum & Wilson (1995). The activation kinetics of I_h were, however, more faithful to

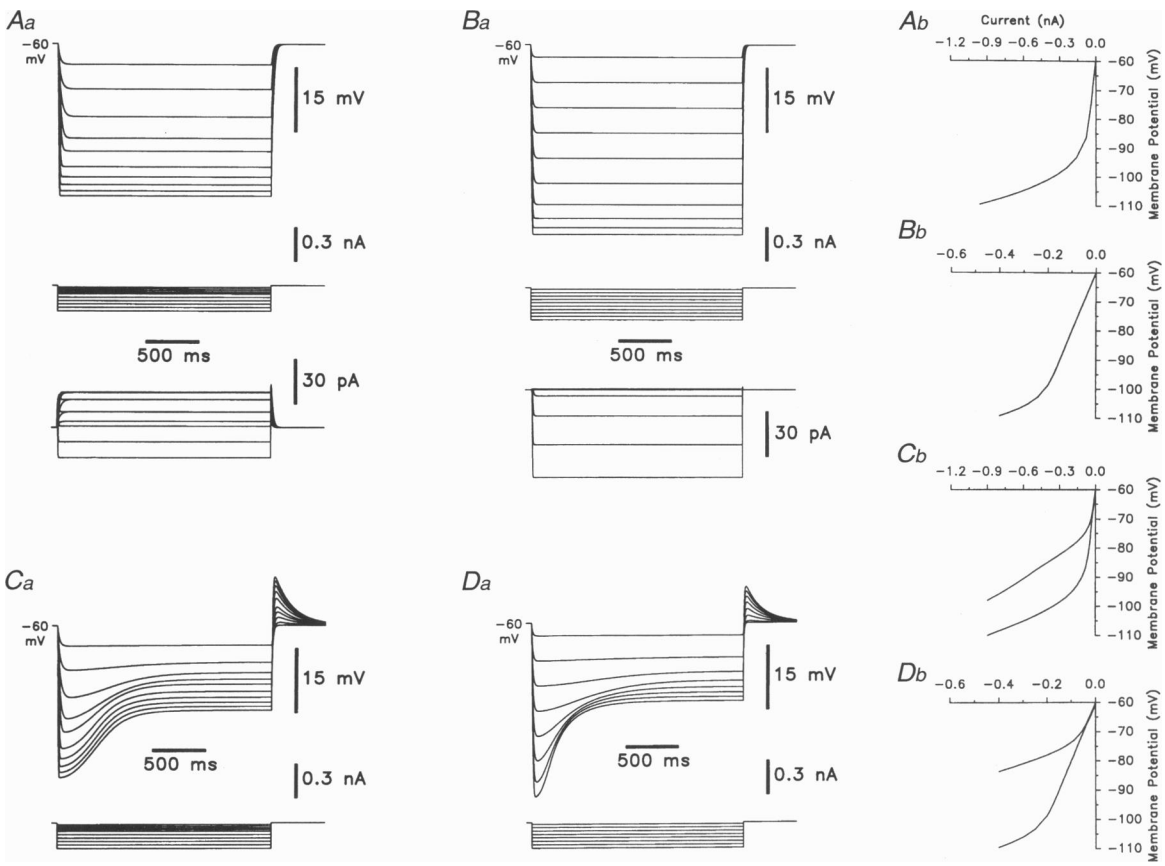

Figure 12. The pattern of anomalous rectification of TC neurones is reproduced by a simple model

A, families of voltage (upper records), injected current step (middle records) and inwardly rectifying K^+ current (I_{KIR}) (lower records) traces demonstrate that anomalous rectification is formed by I_{KIR} (*a*). In this simulation E_K is −95 mV, and I_{KIR} has a first order activation kinetics and a maximal conductance of 100 nS. The model also included I_{Leak} with a conductance of 5 nS. The third quadrant *V–I* relationship has a non-linear structure, and rectification is apparent from membrane potentials more negative than −85 mV (*b*). Anomalous rectification is initially formed by outward I_{KIR}. *B*, a simulation using identical parameters as in *A*, but with a third order activation kinetics for I_{KIR} (*a*), reveals that anomalous rectification is first apparent at potentials close to E_K (*b*). Note the minimal outward current of I_{KIR} with the third order activation kinetics. *C*, the addition of a simulated I_h reveals the full pattern of rectification of the model neurone with I_{KIR} modelled with a first order activation kinetics: a slow depolarizing sag is apparent during the course of negative voltage deviations (*a*). The *V–I* relationship under these conditions demonstrates time-dependent rectification (*b*) (the curves are produced by measurement made at the negative peaks and 10 ms before the offset of voltage deviations). *D*, a third order activation kinetics for I_{KIR} transforms the kinetics of the depolarizing sag (*a*) and the degree of voltage separation between the *V–I* relationships measured at peak and steady-state points (*b*), indicating that the pattern of peak and time-dependent anomalous rectification is influenced by the parameters used to describe I_{KIR}.

those apparent in TC neurones (Tóth & Crunelli, 1992). In a model that contained only I_{Leak} and I_{KIR}, rectification was apparent in third quadrant V–I relationship (Fig. 12*A* and *B*). The voltage at which rectification was first apparent was dependent upon the activation kinetics of I_{KIR}: rectification was expressed at membrane potentials more positive than E_K when a first order activation was used to model I_{KIR} (Fig. 12*Aa* and *Ab*), and at, or more negative than, E_K when third order activation kinetics was employed (Fig. 12*Ba* and *Bb*). These data indicated that anomalous rectification may be initially formed when I_{KIR} is an outward current, and under these circumstances I_{KIR} leads to rectification by acting as a shunt conductance. We constructed a steady-state V–I relationship in simulations where E_K was allowed to vary as a free parameter, in the presence of I_{KIR} modelled with either a first or third order activation kinetics (Fig. 13). These parameter changes revealed that with both first and third order kinetics the voltage at which fast rectification was first apparent obeyed a voltage–E_K relationship. Our experimental data was best approximated by a first order kinetics of I_{KIR} when E_K was set to −90 to −95 mV: in this case the V–I relationship showed a region of maximal slope resistance at potentials similar to those of TC neurones recorded in the presence of ZD 7288 (Fig. 13*B*). When a third order activation kinetics was used, experimental data was best approximated when E_K was set to potentials more positive than −80 mV (Fig. 13*C*). Although these results do not reflect a unique solution, they

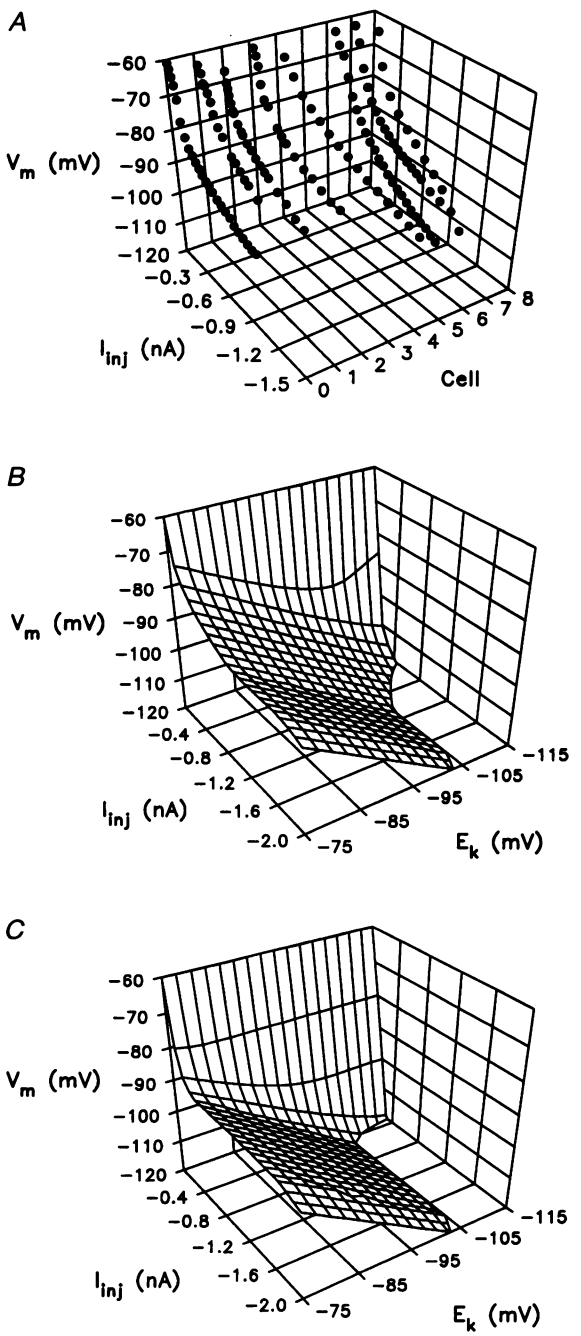

Figure 13. Fast anomalous rectification is dependent upon the activation kinetics of I_{KIR} and E_K

A, third quadrant V–I relationship of a representative group of TC neurones of the VB thalamus recorded in the presence of ZD 7288 (100–300 μM) demonstrate a non-linear structure, with fast rectification apparent from membrane potentials more negative than about −85 mV. Membrane voltage (V_m), is plotted against injected current (I_{inj}) for different neurones (Cell). *B*, computer simulations, formulated with an inwardly rectifying K^+ current (I_{KIR}), (with first order activation kinetics) and with I_{Leak}, demonstrate that the region at which the V–I relationships are first rectified is dependent upon the value of E_K. Membrane voltage (V_m), is plotted against I_{inj} and E_K. Note that with this activation kinetics the V–I relationships formed with an E_K of −90 to −95 mV show the closest correspondence with the experimental data. *C*, simulations made with a third order activation kinetics for I_{KIR} shows a qualitatively similar relationship between the voltage at which the V–I relationships are first rectified and E_K. Note, however, that with these parameters the closest correspondence with experimental data is obtained at values of E_K between −75 and −85 mV.

indicate that in TC neurones I_{KIR} may act to form fast anomalous rectification at potentials more positive than E_K.

By addition of I_h to the model, both fast and time-dependent anomalous rectification was observed (Fig. 12*C* and *D*). The degree of time-dependent (i.e. I_h-mediated) rectification, indicated by the amplitude of the depolarizing sag potential, was influenced by the order of the I_{KIR} activation kinetics, so that when the activation range of I_{KIR} and I_h overlapped (as it is the case for a first order activation of I_{KIR}) the depolarizing sag potential was reduced in amplitude (Fig. 12*C*). In experiments, the application of Ba^{2+} (0·1–2 mM) ($n = 3$) to control neurones linearized peak third quadrant *V–I* relationships and led to the formation of a greater degree of time-dependent rectification (not illustrated). Therefore, blockade or modulation of I_{KIR} will increase the functional expression of I_h when observed under current clamp conditions as a depolarizing sag potential, indicating that I_{Leak}, I_{KIR} and I_h act together to form the pattern of anomalous rectification in TC neurones.

DISCUSSION

The main conclusions of this investigation are as follows. (i) The anomalous rectification properties of TC neurones may be formed by three voltage-activated currents, I_h, I_{KIR} and $I_{h,slow}$. (ii) Under control conditions anomalous rectification has fast and time-dependent components; time-dependent rectification formed by I_h is sensitive to ZD 7288, whilst fast rectification is abolished by Ba^{2+}, indicating that fast rectification is mediated by I_{KIR}. (iii) Computer simulations and experimental observations suggest that I_{KIR} is active at potentials more positive than E_K. (iv) The blockade of I_h and I_{KIR} reveals the presence of a large amplitude, very slowly activating, non-inactivating inward current ($I_{h,slow}$) that is activated from potentials more negative than −90 mV and may represent a novel hyperpolarization-activated membrane current.

Characteristics of I_h

The voltage dependence of I_h was found to be similar to that of slow, hyperpolarization-activated currents exhibited by neurones from other structures (Mayer & Westbrook, 1983; Spain, Schwindt & Crill, 1987; McCormick & Pape, 1990; Soltesz *et al.* 1991; Larkman & Kelly, 1992; Solomon & Nerbonne, 1993; Womble & Moises, 1993). In the present study the activation of I_h was best approximated by the sum of two exponential functions with time constants τ_{fast} and τ_{slow}, both related in a similar manner to membrane voltage, so that they were large at potentials where I_h was first activated and broadly decreased as a function of membrane potential negativity. The description of I_h by the sum of two exponential functions is in contrast with previous analysis in TC neurones of the cat and guinea-pig dorsal lateral geniculate nucleus (McCormick & Pape, 1990; Soltesz *et al.* 1991; Pape, 1994) and in neurones of other structures (Larkman & Kelly, 1992; Soloman, Doyle, Burkhalter & Nerbonne, 1993; Womble & Moises, 1993). However, other investigations of central neurones have indicated that I_h may best be approximated by the sum of two exponential functions (Spain *et al.* 1987; Banks, Pearce & Smith, 1993; Solomon, *et al.* 1993; Solomon & Nerbonne, 1993). Such contrasting data may be explained in several ways. Differences in the frequency at which current records are filtered and digitally sampled have been shown to alter the number of terms required to approximate current data (Solomon & Nerbonne, 1993). It is of interest, therefore, that in TC neurones of the cat and guinea-pig dorsal lateral geniculate nucleus, the activation and deactivation of I_h shows considerable variation from a fit with mono-exponential terms (see Fig. 3 of McCormick & Pape, 1990), suggesting the presence of kinetically distinct components. The present kinetic description of I_h suggests that two distinct currents, carried by different ions, are activated by hyperpolarization in TC neurones. We cannot exclude this possibility as we have not analysed the deactivation of I_h. However, recordings with potassium chloride electrodes, a procedure shown to alter E_{Cl} in TC neurones (Crunelli *et al.* 1988), produced results similar to those obtained with potassium acetate electrodes, and the application of Ba^{2+}, which blocked fast anomalous rectification, did not simplify the activation kinetics of I_h. Furthermore, the sum of two exponential functions best approximated I_h waveform over the entire voltage range tested; at relatively positive values of this range, instantaneous *I–V* relationships were linear and so may be considered minimally contaminated by the current(s) responsible for fast anomalous rectification. These data suggest that the current(s) underlying fast rectification do not introduce a time-dependent component that interfered with the kinetic analysis of I_h, in contrast to that indicated for neurones of the basolateral amygdala (Womble & Moises, 1993). Thus, we suggest that the bi-exponential description of I_h represents the activation of kinetically distinct components carried by the same ionic species. It remains to be established whether these properties are a reflection of multiple gating processes of the same population of ion channels, or whether distinct populations of ion channels are involved.

Under current- and voltage clamp conditions, time-dependent anomalous rectification was found to be blocked by ZD 7288. The selectivity of this effect is suggested by the observation that fast anomalous rectification and fast and time-dependent outward rectification were minimally affected. The long onset of action, the apparent irreversible nature and lack of use dependence of the blockade of I_h by ZD 7288 observed in the present study are consistent with an intracellular site of action of this compound, as was originally shown by Harris & Constanti (1995).

Fast anomalous rectification

V–I and *I–V* relationships demonstrated fast anomalous rectification that was apparent from membrane potentials more negative than −85 mV and was not mediated by I_h. Fast anomalous rectification has been suggested to be mediated by I_{KIR} in central neurones (see Introduction for

references), and found to be sensitive to Ba^{2+} and Cs^{+}, as originally described for non-neuronal cells (Gay & Stanfield, 1977; Hagiwara *et al.* 1976, 1978; Standen & Stanfield, 1978). We observed that Ba^{2+} (100 μM) led to a blockade of anomalous rectification, accompanied by a membrane potential depolarization or tonic inward current. No time-dependent effects of Ba^{2+} were observed in the majority of neurones, whilst in some neurones under voltage clamp conditions the amplitude of inward currents decreased during the first 0·1 to 3 s of a negative voltage step, and under current clamp conditions a time-dependent increase in the amplitude of negative voltage deviations was observed. The time-dependent effects of Ba^{2+} on I_{KIR} are known to decrease over a concentration range between 1 and 100 μM in central neurones (Uchimura *et al.* 1989). The differential time dependence observed may suggest that the final concentration of Ba^{2+} present in the environment of individual neurones was variable, perhaps reflecting a concentration gradient at different depths in tissue slices. As rectification was apparent at around −85 mV under current clamp conditions, we reasoned it may initially be formed by I_{KIR} activated at membrane potentials more positive than E_K, as E_K has been estimated to be approximately −95 mV in TC neurones (Crunelli *et al.* 1988; Williams *et al.* 1995). Furthermore, Ba^{2+}-sensitive conductances in central neurones have been shown to be first activated at membrane potentials of, or more positive than, −85 mV (Uchimura *et al.* 1989; Sutor & Hablitz, 1993; Womble & Moises, 1993) and I_{KIR} first activated at potentials up to 60 mV more positive than E_K in retinal cells (Dong & Werblin, 1995). Simulations using a model containing I_{Leak} and I_{KIR} produced steady-state V–I relationships similar to those constructed experimentally, with a region of steep slope and anomalous rectification. The steep slope region was found to be defined by outward I_{KIR} and I_{Leak}, and rectification was first apparent at potentials more positive than E_K. These data, therefore, indicate that the blockade of outward I_{KIR} may be responsible for the tonic inward current produced by application of Ba^{2+} in the experiments, and that the form of I_{KIR} in TC neurones of the cat VB thalamus may be described as a weak inward rectifier (Lu & McKinnon, 1994). A Ba^{2+}-mediated blockade of I_{Leak} (cf. McCormick & Pape, 1990) may, however, have contributed to the effects of this ion, although our data indicates that this is not the dominant mode of action of Ba^{2+} in TC neurones of the cat VB thalamus. Taken together, these results represent the first electrophysiological evidence on the presence and action of inwardly rectifying K^{+} channels in TC neurones, while the expression of mRNA from different KIRs and GIKRs in the thalamus has recently been reported (Karschin, Dißmann, Stühmer & Karschin, 1996).

In a subset of neurones, the most prominent feature of anomalous rectification recorded under current clamp conditions in the continuous presence of ZD 7288 was the presence of a time-dependent increase in input resistance, expressed at potentials more negative than −85 mV. Such activity, resembled the time-dependent blockade of anomalous rectification observed in the presence of Ba^{2+} Under voltage clamp conditions, such activity was apparent as fading of the instantaneous inward current, following the settling of capacative artifacts. The similarity between the activity apparent in the absence and presence of Ba^{2+}, suggests that these effects may be mediated by an inactivation of I_{KIR}. Previous investigations have indicated a decay of inward currents through I_{KIR} in neuronal (Yamaguchi, Nakajima, Nakajima & Stanfield, 1990) and non-neuronal cells (Standen & Stanfield, 1979). Although we have not analysed the properties of inactivation of I_{KIR}, the presence of this behaviour in a subset of neurones suggests that the properties of I_{KIR} are distinct between neurones. Note that this activity is different from the time-dependent increase in input resistance underlying the voltage and temporal amplification of synaptic potentials observed in other TC neurones and described in the accompanying paper (Williams, Tóth, Turner, Hughes & Crunelli, 1997), since the latter is mediated by the influence of the 'window' component of I_T.

Characteristics of the very slowly activating inward current

Under control conditions the slow exponential terms used to describe I_h were often observed to be a non-linear function of the membrane potential, first decreasing and then increasing with membrane negativity. One explanation for such behaviour is that a qualitatively different form of inward current, with slow activation kinetics, is expressed in TC neurones. Indeed, following the blockade of I_h with ZD 7288, a very slow inward current, which we have termed $I_{h,slow}$, was apparent in some neurones but not in others. The extracellular application of Ba^{2+} blocked fast anomalous rectification and either augmented, or revealed the presence of, $I_{h,slow}$ in these groups, respectively. We suggest that $I_{h,slow}$ represents a mixed cationic current, as the reversal potential of its tail currents was found to lie between −50 and −65 mV, and the form of current and reversal of tail currents were not different between neurones impaled with potassium acetate or potassium chloride electrodes. Moreover, since $I_{h,slow}$ was sensitive to high concentrations of Cs^{+} (5 mM), in all characteristics apart from activation kinetics and voltage dependence $I_{h,slow}$ resembles the hyperpolarization-activated mixed cationic currents described for other neurones (Mayer & Westbrook, 1983; Spain *et al.* 1987; McCormick & Pape, 1990; Soltesz *et al.* 1991; Banks *et al.* 1993).

We suggest that $I_{h,slow}$ may represent a distinct ionic current. There are several lines of evidence that support this view, the details and caveats of which are outlined below.

(i) $I_{h,slow}$ may not be formed by the pharmacological agents used for its isolation. Previous analysis has indicated that the activation curve of I_f in dissociated cardiac cells is shifted toward more negative voltages by ZD 7288 without changes in the activation time constant of this current

(BoSmith *et al.* 1993). Results from the present investigation, however, indicate that the activation kinetics of $I_{h,slow}$ are at least threefold slower than those of I_h, an effect incompatible with $I_{h,slow}$ being formed by a simple change in the voltage dependence of I_h by ZD 7288 in TC neurones. Similarly, in other central neurones Harris & Constanti (1995) have demonstrated that the application of ZD 7288 leads to the appearance of an inward current with very slow activation kinetics following intense (more negative than −90 mV) membrane hyperpolarization. These authors suggest that this slow inward current is generated by the voltage-dependent relief of blockade of I_h by ZD 7288 (i.e. a decrease in the ability of ZD 7288 to block I_h at very negative membrane potentials). In the present study we have investigated the conductance changes accompanying the deactivation of $I_{h,slow}$, and demonstrated that the voltage dependence and time course of these effects are more compatible with the deactivation of a slow membrane current, rather than a voltage-dependent relief of I_h blockade by ZD 7288.

(ii) Ba^{2+} augments the amplitude of $I_{h,slow}$, but does not change the characteristics of I_h. If I_h and $I_{h,slow}$ were to represent current flow through the same ion channels, the properties of which are modifiable by ZD 7288, it would be anticipated that $I_{h,slow}$ and I_h would be affected by Ba^{2+} in a similar manner. Ba^{2+}, however, did not change the properties of I_h, whilst either augmenting the amplitude of, or revealing, $I_{h,slow}$ when co-applied with ZD 7288. We suggest that these data indicate that the channels responsible for the formation of $I_{h,slow}$ may be independent from those forming I_h and located at sites electrotonically remote to the recording site. It is, therefore, an improvement of voltage- and space clamp that leads to the modulation of the properties of $I_{h,slow}$ by Ba^{2+}. Indeed, simulation studies have indicated that the presence of fast and time-dependent rectification will render the electrotonic structure of neurones highly voltage-dependent (Spain *et al.* 1987; Wilson, 1992). Thus, the facilitation of $I_{h,slow}$ following the blockade of I_h and I_{KIR} may indicate a substantial dendritic location of the ion channels responsible for the formation of $I_{h,slow}$.

(iii) Electrophysiological evidence for the distinction of $I_{h,slow}$. We have recorded I_h with similar properties in each neurone under control conditions, whilst $I_{h,slow}$ was not apparent in every neurone exposed to ZD 7288 alone. Moreover, kinetic analysis, using suitably long duration voltage steps (5–15 s) of the current(s) responsible for time-dependent anomalous rectification under control conditions, revealed the presence of long time constants at membrane potentials more negative than −90 mV. If such rectification was mediated by I_h alone, such analysis should have revealed a progressive reduction in activation time constant with membrane potential negativity.

These data, together with the lower sensitivity of $I_{h,slow}$ to 3 mM Cs^+, are supportive of the notion that $I_{h,slow}$ may represent a novel anomalous rectifier, and provide evidence that warrants further detailed investigations.

Physiological implications

The different forms of anomalous rectification described for TC neurones of the VB thalamus may be considered to act together in the formation and control of these neurones' electroresponsiveness at hyperpolarized potentials. Since the amplitude and kinetics of the depolarizing sag apparent during negative voltage deviations is controlled by the concerted actions of I_{KIR}, I_h and I_{Leak}, the duration and amplitude of inhibitory postsynaptic potentials will be influenced by these currents. In TC neurones, $GABA_A$ and/or $GABA_B$ receptor-mediated inhibitory postsynaptic potentials have been shown to lead to the burst firing of action potentials driven by low-threshold Ca^{2+} potentials, as a consequence of the time- and voltage-dependent removal of inactivation of I_T (Crunelli, *et al.* 1988, 1989; Steriade *et al.* 1993). Therefore, modulation of I_{KIR}, I_h and I_{Leak} by the neurotransmitters of the ascending activating systems (McCormick, 1992) will affect the amplitude and kinetics of synaptic potentials generated in, and as a consequence the output of, TC neurones. Indeed, if $I_{h,slow}$ has a substantial dendritic location, as indicated by our observations, it will be ideally positioned to influence the amplitude and duration of slow and summated inhibitory postsynaptic potentials as the GABA-containing synapses of the nucleus reticularis thalami are found on relatively distal dendrites of TC neurones (Shermann & Koch, 1986). As the nucleus reticularis thalami neurones are involved in the generation of network-driven oscillations of TC neurones during, for example, sleep spindles or spike and wave discharges (Steriade, Deschênes, Domich & Mulle, 1985; Steriade, *et al.* 1993; Bal, von Krosigk & McCormick, 1995), $I_{h,slow}$ may play a critical role in formation and control of thalamo-cortical output.

Bal, T., von Krosigk, M. & McCormick, D. M. (1995). Role of the ferret perigeniculate nucleus in the generation of synchronized oscillations *in vitro*. *Journal of Physiology* **483**, 665–685.

Banks, M. I., Pearce, R. A. & Smith, P. H. (1993). Hyperpolarization-activated cation current (I_h) in neurons of the medial nucleus of the trapezoid body: voltage-clamp analysis and enhancement by norepinephrine and c-AMP suggest a modulatory mechanism in the auditory brain stem. *Journal of Neurophysiology* **70**, 1420–1432.

BoSmith, R. E., Briggs, I. & Sturgess, N. C. (1993). Inhibitory action of zeneca ZD 7288 on whole-cell hyperpolarization activated inward current (I_f) in guinea-pig dissociated sinoatrial cells. *British Journal of Pharmacology* **110**, 343–349.

Constanti, A. & Galvan, M. (1983). Fast inward-rectifying current accounts for anomalous rectification in olfactory neurones. *Journal of Physiology* **335**, 153–178.

Crunelli, V., Haby, M., Jassik-Gershenfeld, D., Leresche, N. & Pirchio, M. (1988). Cl^-- and K^+-dependent inhibitory postsynaptic potentials evoked by interneurones of the rat lateral geniculate nucleus. *Journal of Physiology* **399**, 153–176.

Crunelli, V., Lightowler, S. & Pollard, C. E. (1989). A T-type Ca^{2+} current underlies low-threshold Ca^{2+} potentials in cells of the cat and rat lateral geniculate nucleus. *Journal of Physiology* **413**, 543–561.

Dong, C.-J. & Werblin, F. S. (1995). Inwardly rectifying conductances can accelerate the hyperpolarizing response in retinal horizontal cells. *Journal of Neurophysiology* **74**, 2258–2265.

Finkel, A. S. & Redman, S. (1984). Theory and operation of a single micro-electrode voltage clamp. *Journal of Neuroscience Methods* **11**, 101–127.

Gay, L. A. & Stanfield, P. R. (1977). Cs^+ causes a voltage-dependent block of inward K currents in resting skeletal muscle fibres. *Nature* **267**, 169–170.

Hagiwara, S., Miyazaki, S., Moody, W. & Patlak, J. (1978). Blocking effects of barium and hydrogen ions on the potassium current during anomalous rectification in the starfish egg. *Journal of Physiology* **279**, 167–185.

Hagiwara, S., Miyazaki, S. & Rosenthal, N. P. (1976). Potassium current and the effects of cesium on this current during anomalous rectification of the egg cell membrane of a starfish. *Journal of General Physiology* **67**, 612–638.

Harris, N. C & Constanti, A. (1995). Mechanism of block by ZD 7288 of the hyperpolarization-activated inward rectifying current in guinea-pig substantia nigra neurons *in vitro*. *Journal of Neurophysiology* **74**, 2366–2378.

Hu, B. (1995). Cellular basis of temporal synaptic signalling – an *in vitro* electrophysiological study in rat auditory thalamus. *Journal of Physiology* **483**, 167–182.

Karschin, C., Dißmann, E., Stühmer, W. & Karschin, A. (1996). IRK(1–3) and GIRK(1–4) inwardly rectifying K^+ channels mRNAa are differentially expressed in the adult rat brain. *Journal of Neuroscience* **16**, 3559–3570.

Larkman, P. M. & Kelly, J. S. (1992). Ionic mechanisms mediating 5-hydroxytryptamine- and noradrenaline-evoked depolarization of adult rat facial motoneurones. *Journal of Physiology* **456**, 473–490.

Lu, Z. & McKinnon, R. (1994). Electrostatic tuning of Mg^{2+} affinity in an inward-rectifier K^+ channel. *Nature* **371**, 243–246.

McCormick, D. A. (1992). Neurotransmitter actions in the thalamus and cerebral cortex and their role in neuromodulation of thalamocortical activity. *Progress in Neurobiology* **39**, 337–388.

McCormick, D. A. & Pape, H.-C. (1990). Properties of a hyperpolarization-activated cation current and its role in rhythmic oscillation in thalamic relay neurons. *Journal of Physiology* **431**, 291–318.

Mayer, M. L. & Westbrook, G. L. (1983). A voltage-clamp analysis of inward (anomalous) rectification in mouse spinal sensory ganglion neurones. *Journal of Physiology* **340**, 19–45.

Nisenbaum, E. S. & Wilson, C. J. (1995). Potassium currents responsible for inward and outward rectification in rat neostriatal spiny projection neurons. *Journal of Neuroscience* **15**, 4449–4463.

Pape, H.-C. (1994). Specific bradycardiac agents block the hyperpolarization-activated cation current in central neurons. *Neuroscience* **59**, 363–373.

Shermann, S. M. & Koch, C. (1986). The control of retinogeniculate transmission in the mammalian lateral geniculate nucleus. *Experimental Brain Research* **63**, 1–20.

Solomon, J. S., Doyle, J. F., Burkhalter, A. & Nerbonne, J. M. (1993). Differential expression of hyperpolarization-activated currents reveals distinct classes of visual cortical projection neurons. *Journal of Neuroscience* **13**, 5082–5091.

Solomon, J. S. & Nerbonne, J. M. (1993). Two kinetically distinct components of hyperpolarization-activated current in rat superior colliculus-projecting neurons. *Journal of Physiology* **469**, 291–313.

Soltesz, I., Lightowler, S., Leresche, N., Jassik-Gerchenfeld, D., Pollard, C. E. & Crunelli, V. (1991). Two inward currents and the transformation of low frequency oscillations of rat and cat thalamocortical cells. *Journal of Physiology* **441**, 175–197.

Spain, W. J., Schwindt, P. C. & Crill, W. E. (1987). Anomalous rectification in neurons from cat sensorimotor cortex *in vitro*. *Journal of Neurophysiology* **57**, 1555–1576.

Staley, K. (1994). The role of an inwardly rectifying chloride conductance in postsynaptic inhibition. *Journal of Neurophysiology* **72**, 273–284.

Standen, N. B. & Stanfield, P. R. (1978). A potential- and time-dependent blockade of inward rectification in frog skeletal muscle fibres by barium and strontium ions. *Journal of Physiology* **280**, 169–191.

Standen, N. B. & Stanfield, P. R. (1979). Potassium depletion and sodium block of potassium currents under hyperpolarization in frog sartorious muscle. *Journal of Physiology* **294**, 497–520.

Steriade, M., Curró Dossi, R. & Nuñez, A. (1991). Network modulation of a slow intrinsic oscillation of cat thalamocortical neurons implicated in sleep delta waves: cortical induced synchronization and brainstem cholinergic suppression. *Journal of Neuroscience* **11**, 3200–3217.

Steriade, M., Deschênes, M., Domich, L. & Mulle, C. (1985). Abolition of spindle oscillations in thalamic neurons disconnected from nucleus reticularis thalami. *Journal of Neurophysiology* **54**, 1473–1497.

Steriade, M., McCormick, D. A. & Sejnowski, T. (1993). Thalamocortical oscillations in the sleeping and aroused brain. *Science* **262**, 679–685.

Sutor, B. & Hablitz, J. J. (1993). Influence of barium on rectification in rat neocortical neurons. *Neuroscience Letters* **157**, 62–66.

Tóth, T. I. & Crunelli, V. (1992). Computer simulation of the pacemaker osillation of thalamocortical cells. *NeuroReport* **3**, 65–68.

Turner, J. P., Anderson, C. M., Williams, S. R. & Crunelli, V. (1997). Morphology and membrane properties of neurones in the cat ventrobasal thalamus *in vitro*. *Journal of Physiology* **505**, 707–726.

Uchimura, N., Cherubini, E. & North, R. A. (1989). Inward rectification in rat nucleus accumbens neurons. *Journal of Neurophysiology* **62**, 1280–1286.

VanBogaert, P. P., Goethals, M. & Simoens, C. (1990). Use- and frequency-dependent blockade by UL-FS 49 of the I_f pacemaker current in sheep cardiac purkinje fibres. *European Journal of Pharmacology* **187**, 241–256.

Williams, S. R. & Crunelli, V. (1996). Fast and time-dependent anomalous rectification in thalamocortical neurones. *Society for Neuroscience Abstracts* **22**, 46.6.

Williams, S. R., Tóth, T. I., Turner, J. P., Hughes, S. W. & Crunelli, V. (1997). The 'window' component of the low threshold Ca^{2+} current produces input signal amplification and bistability in cat and rat thalamocortical neurones. *Journal of Physiology* **505**, 689–705.

Williams, S. R., Turner, J. P. & Crunelli, V. (1995). Gamma-hydroxybutyrate promotes oscillatory activity of rat and cat thalamocortical neurons by a tonic $GABA_B$ receptor-mediated hyperpolarization. *Neuroscience* **66**, 133–141.

Wilson, C. J. (1992). Dendritic morphology, inward rectification, and the functional properties of neostriatal neurones. In *Single Neuron Computation*, ed. McKenna, T., Davis, J. & Zornetzer, S. J., pp. 141–171. Academic Press, London.

WOMBLE, M. D. & MOISES, H. C. (1993). Hyperpolarization-activated currents in neurons of the rat basolateral amygdala. *Journal of Neurophysiology* **70**, 2056–2065.

YAMAGUCHI, K., NAKAJIMA, Y., NAKAJIMA, S. & STANFIELD, P. R. (1990). Modulation of inwardly rectifying channels by substance P in cholinergic neurones from rat brain in culture. *Journal of Physiology* **426**, 499–520.

Acknowledgements

We would like to thank Tim M. Gould and Caroline M. Anderson for assistance with some of the experiments, and Bob M. Jones for photography. The support of The Wellcome Trust (grant no. 34089) is gratefully acknowledged. S.R.W. and S.W.H. were Wellcome Prize Students.

Authors' present addresses

S. R. Williams: Reed Neurological Research Center, UCLA School of Medicine, Los Angeles CA 90024, USA.

J. P. Turner: Department of Visual Science, Institute of Opthalmology, London EC1V 9EL, UK.

Author's email address

V. Cruneli: crunelli@cardiff.ac.uk

Received 28 April 1997; accepted 12 August 1997.